2000 years of event sedimentation in Lake Iseo (Italian Alps) under the influence of floods, earthquakes and human activities

William Rapuc[1], Fabien Arnaud[1], Pierre Sabatier[1], Flavio S. Anselmetti[2], Andrea Piccin[3], Laura Peruzza[4], Antoine Bastien[1], Laurent Augustin[5], Edouard Régnier[6], Jérôme Gaillardet[7] & Ulrich Von Grafenstein[6]

[1]Univ. Savoie Mont Blanc, CNRS, EDYTEM, 73000 Chambéry, France

[2]Institute of Geological Sciences and Oeschger Centre for Climate Change Research, University of Bern, Baltzerstrasse 1+3, 3012 Bern, Switzerland

[3]Regione Lombardia, D.G. Territorio e Urbanistica, Struttura Sistema Informativo Territoriale, 20124 Milano, Italy

[4]Istituto Nazionale di Oceanografia e di Geofisica Sperimentale—OGS, Sgonico, TS, Italy

[5]Division technique de l'INSU, Centre de Carottage et de Forage National, CNRS, France

[6]LSCE, Université de Versailles Saint-Quentin, Commissariat à l'Energie Atomique–CNRS, 91198 Gif-sur-Yvette, France

[7] Université de Paris, Institut de physique du globe de Paris, CNRS, Paris F-75005, France

Corresponding Author:

William Rapuc

UMR CNRS 5204 Environnements, Dynamiques et Territoires de la Montagne (EDYTEM)

Université Savoie Mont Blanc, Campus scientifique,

73376 Le Bourget du Lac cedex, France

william.rapuc@univ-smb.fr

Abstract

Few of the large Southern peri-alpine lakes have been studied with a sedimentological approach in their deep basin to understand the dynamics of their long-term sedimentation due, among other factors, to the high complexity of the coring in such deep lakes. In 2018, a 15.5 m-long sediment section was retrieved from the deep basin of Lake Iseo (Italy) at 251 m of water depth. Seismic survey associated to a multi-proxy approach with sedimentological and geochemical analyses, reveals a high number of event layers that corresponds to 61.4 % of the total sedimentation during the last 2000 years. The great heterogeneity of textures, colours, and grain-size distribution between the different types of event layers can be explained by the high number of potential sources of sediment inputs in this large lake system. By combining proxies for sediment source with transport processes, we were able to distinguish: i) flood events, and ii) destabilisations of slopes and deltas due to an increase of the sediment load and/or to seismic shaking. From a thorough comparison with both, the regional climatic fluctuations, and the human activity in the watershed, it appears that periods of high sediment remobilization can be linked to a previous increase in Critical Zone erosion in the watershed mainly under human forcing. Hence, even in large catchments, human activities play a key role on erosion processes and on sediment availability, disrupting the recording of the Critical Zone functioning in such lacustrine archive.

Keywords

Lake sediment, Flood frequency, Earthquake records, Human activity, Erosion

1. Introduction

The Critical Zone (CZ) is defined as the thin active layer at the Earth's surface where occur all energy and matter exchanges that are necessary to sustain life (Banwart et al., 2013). Erosion is one of the most efficient mechanism of matter transfer across the CZ. As such it carries information about most of the triggering mechanisms of CZ changes: climate, human activities and geodynamics, all acting and evolving following different time-paces. At the end of watersheds, sedimentation occurs in depositional sinks, allowing the recording of CZ functioning. However, CZ is impacted by human activities combined with climatic fluctuations notably through the cycle of erosion (Lu et al., 2017; Syvitski et al., 2005) leading to a major concern since excessive erosion threatens the sustainability of biodiversity, reduces arable lands fertility and increases natural hazard harmfulness (Steffen et al., 2015).

Recently, many studies based on natural archives have shown how human activities in watersheds played a key role in the erosion and in sediment transport processes (Arnaud et al., 2016; Brisset et al., 2017; Doyen et al., 2013; Giguet-Covex et al., 2012; Rapuc et al., 2019; Zádorová et al., 2013). Expanding grazing, agricultural activities and the often-associated deforestation all induced a general destabilization of slopes and an increase in sediment input towards depositional sinks (Edwards and Whittington, 2001). In the Alps, human activities have increased erosion from the end of the Neolithic at ~4 ka cal BP and even more significantly at the beginning of the Iron Age and during the Roman Period (Andrič et al., 2020; Bajard et al., 2016; Giguet-Covex et al., 2011; Joannin et al., 2014; Rapuc et al., 2018; Regattieri et al., 2019; Vannière et al., 2013). Even if lake sediments provide a continuous and well-preserved natural archive of such variations, strong and sudden inputs of sediment can disturb this record. Indeed, sediment availability in small lake basins and watersheds plays a key role in the sensitivity of the lake to record extreme events such as floods, avalanches or earthquakes (Brisset et al., 2017; Fouinat et al., 2018; Rapuc et al., 2018; Wilhelm et al., 2016). It has been shown that human-triggered soil destabilisation may lead to an apparent increase in flood frequency by increasing the amount of sediment available for erosion (Brisset et al., 2017; Fouinat et al., 2017; Giguet-Covex et al., 2012). Similarly, climate- or human-triggered rise in erosion result in sediment inputs in a lake basin, increasing the sensitivity of the lake to record earthquake shaking while excess of sediment input tends to destabilise slopes and deltas (Rapuc et al., 2018; Wilhelm et al., 2016). By modifying the cycles of erosion and sediment transport processes, human activities impact the sedimentation in the different sinks and thus the recording of the functioning of the CZ in watersheds.

However, such studies were all led in small-scale lakes and catchment areas. It is thus necessary to address the question in the case of a large lowland lake basin fed by a large catchment area. Such lakes are particularly promising targets to reconstruct past hydroclimate changes at a regional scale (Arnaud et al., 2016). Large lakes have been underused until now due to technical difficulties to retrieve long-enough cores. Compared to smaller water bodies, large lakes are also most challenging to study due to the (i) multiple sediment sources linked to multiple inflows, (ii) an inhomogeneity of the in-lake biogenic sedimentation at different water depth and location, and (iii) several processes that can impact the continuous sedimentation such as floods, earthquakes, or remobilisation of sediment after an overloading on slopes and deltas (Sauerbrey et al., 2013; Sturm and Matter, 1978); making more difficult the interpretation of the erosion signal.

Here, thanks to a new coring system, we present a novel study with a long sediment core from a large peri-alpine lake that records extreme local and regional geodynamical events linked to human and to climate forcing. This sediment sequence was sampled in the deep basin of Lake Iseo at the downstream end of the Val Camonica valley in Northern Italy. By using a multi-proxy approach, combining a seismic survey with sedimentological and geochemical analyses, we identified a high number of event layers related to different triggers deposited during the last 2000 years. We document that the fluctuations in numbers and intensities of these events (floods, earthquakes) are related to sediment availability in the deep basin and in the lake catchment. Human activities are well-documented in the Val Camonica (e.g. Anati and Cittadini, 1994; Gehrig, 1997; Marziani and Citterio, 1999; Pini, 2002; Pini et al., 2016) and various regional paleoclimate records already exist (Büntgen et al., 2011; Joannin et al., 2014; Vannière et al., 2013). A thorough comparison with both the regional climate and the human activity in the watershed from the Roman period onward is presented to understand how human forcing impacts the event layers record through CZ erosion.

2. Study site

The Italian Alps in Northern Italy host four large lowland lakes, from the Easternmost Lake Garda to the Westernmost Lake Maggiore (**Fig. 1A**). All these lakes present deep basins probably related to the Messinian entrenchment (Bini et al., 1978). Lake Iseo (45°44.205'N; 10°4.340'E) is located in Lombardy, North of the Po plain (**Fig. 1A**), at the Southern end of the Val Camonica valley at an altitude of 185 m a.s.l (above sea level). Lake Iseo (Latin name "Sebino") is, with a length of 25 km and a surface area of 60.9 km^2, the smallest of these four perialpine lakes. The depression that hosts the lake corresponds to a Miocene canyon that was reshaped and re-eroded by several glacier advances during the Pleistocene epoch and filled by Quaternary sediments (Bini et al., 1978). Lake Iseo is a meromictic lake (Ambrosetti and Barbanti, 2005; Salmaso et al., 2003) with the last confirmed mixing of the deep water at the beginning of the 1980s (Salmaso et al., 2003). From then, the oxygen concentration have decreased in the deep water and conditions of permanent anoxia developed during the 1990s. Instrumental data provided by A.R.P.A (http://arpalombardia.it/) indicates that the limit of the hypolimnion is located in water depths between 80 and 100 m. At these depths, the oxygen saturation and pH values decrease sharply, while dissolve calcium concentration increases.

Lake Iseo bathymetry shows two sub-basins separated by Monte Isola, the largest island in an Italian lake (**Fig. 1B**). The smaller basin, the Sale Marasino Basin, is 100 m deep and separated from the main basin by the Monte Isola plateau in its northern part. The Holocene sedimentation of this sub-basin and the plateau were already studied (Lauterbach et al., 2012; Rapuc et al., 2019). The deep basin is 251 m deep and is located West of Monte Isola (**Fig. 1B**).

The Oglio river, which begins in the Adamello Massif, is the main tributary and the unique outlet of Lake Iseo (**Fig. 1B**). This river drains a large watershed (1,842 km^2) with a maximum elevation of 3539 m a.s.l in the Adamello Massif in the Northern part of Val Camonica and a mean altitude of 1400 m a.s.l (Garibaldi et al., 1999). The watershed of Lake Iseo extends up to 60 kilometres Northwards into the Val Camonica valley and only several kilometres to the East and West of the lake (Lauterbach et al., 2012). It is mainly composed of Triassic, Jurassic and Cretaceous limestones and marlstones in the Southern part, associated with Permian sandstones. In the Northern part of the Val Camonica, close to the Periadriatic seam, metamorphic rocks linked to the Alpine orogeny with Tertiary tonalites, granodiorites and quartzodiorites are outcropping. The Val Camonica is well known for its abundance of rock carvings that are registered on the UNESCO World Heritage List. These archaeological evidences provide indications of human presence in the Iseo region since the Mesolithic period (9000–6000 BC). Human settlements, located around the lake and in the Southern-end of the Val Camonica, North of Lake Iseo, dated from Camuni and Roman periods, were identified through numerous archaeological studies (Condina, 1986 and references therein). Several palynological and charcoal studies were conducted in the watershed of Lake Iseo, at different altitudes, from peat bog and small lakes sediments. They are summarized in a recent synthesis (Pini et al., 2016) establishing the evolution of human activities in the lake catchment. This summary indicates that the first trace of agricultural practices are dated to the Neolithic periods (Gehrig, 1997).

The Val Camonica valley and more broadly the North-Eastern part of the Italian Alps are characterised by moderate to high seismic hazards on the national and international maps (MPS WG, 2004; Wiemer et al., 2015; Giardini et al., 2013; Pagani et al, 2018). The tectonic setting is the result of complex collisional and post-collisional phases of the Alpine orogeny (Piaz et al., 2003): the actual crustal shortening in the area is estimated to ~1 $mmyr^{-1}$ (Serpelloni et al., 2005), and several devastating earthquakes have been recorded in the last millennium (**Fig. 1A**; for the most updated Italian earthquake catalogue see Rovida et al, 2020; 2019, hereafter quoted as CPTI15). Two strong historical events occurred in 1117 and 1222 AD, South-Eastward of the study area, have been already recognized in some lake-sediment sequences (Lauterbach et al., 2012 for Iseo; Fanetti et al., 2008 for Como lake). The local seismic activity (magnitude M<6) is ascribed to fold-and-thrust systems, mainly WSW-ENE oriented, blind faults toward the Po Plain, and NNE-SSW oriented in the Garda Lake area (Livio et al., 2009; see references also in DISS Working Group, 2018).

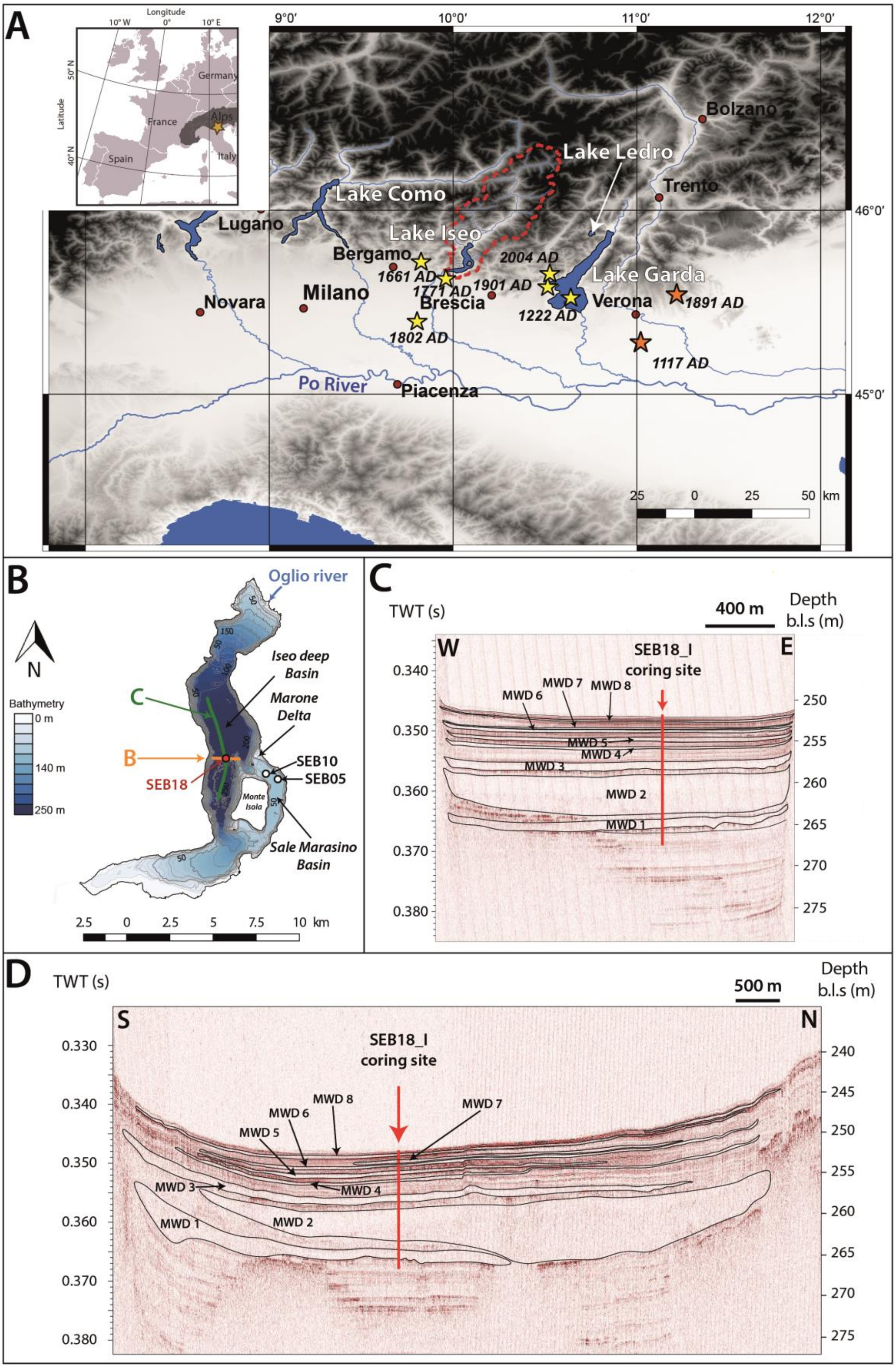

Figure 1 - Lake Iseo location and settings. (A) Locations of Lake Iseo (Italy), its watershed (red dotted line) and the different lakes of the Italian Southern Alps: Lake Como, Lake Garda, and Lake Ledro. The orange and yellow stars correspond to the

location of historic seismic events with a Magnitude ≥ 6 and < 6, respectively. (B) Lake Iseo Bathymetric map associated with the description of the different morphological features and the different coring sites. Seismic profiles W-E (C) and S-N (D) oriented across the deep basin showing the coring site location (vertical red line) and the principal generations of mass wasting layers (MWD, coloured lines). The depth of the seismic profile is expressed in metres below lake surface (m b.l.s.), assuming a mean P-wave velocity of 1450 m.s^{-1} in water and sediments.

3. Materials and Methods

3.1. Seismic survey

To study the long-term evolution of the CZ in the Val Camonica, it is necessary to work on a sediment section fed by the main tributary of the valley, the Oglio river. The two previous studies made on sediment cores from Lake Iseo (**Fig. 1B**) were retrieved from the Sale Marasino basin (SEB05&06) and the Monte Isola Plateau (SEB10), which are not influenced by the main sediment inputs of the Oglio river (Lauterbach et al., 2012; Rapuc et al., 2019). A high-resolution seismic reflection survey using a broad-band (300 – 2400 Hz) single-channel boomer device had been conducted on Lake Iseo in 2002 (Bini et al., 2007). However, these data did not provide sufficient resolution to understand the most recent sediment infilling of the deep lake basin. A medium-resolution seismic reflection survey was conducted on the deep basin in July 2018 to select a suitable coring site, minimizing the amount of reworked sediment and presenting the thinnest instantaneous mass wasting layers (MWD). For this survey, ≈ 51 km of 3.5 kHz pinger (Geoacoustics) single-channel data were acquired with a shooting interval of 500 ms and recorded the SEG-Y data with a sample frequency of 24 kHz. A bandpass filter (1500 – 6500 Hz) was applied. The coring location, SEB18_I (45° 43.536'N ; 10° 3.888'E), was selected in the centre of the deep basin at the intersection of two perpendicular seismic lines, North-West of Monte Isola by 251 m water-depth (**Fig. 1B**). This area is protected from the sediment input from the Marone delta by the ridge North-West of Monte Isola and is supposed to be only influenced by the sediment input from the Oglio river and from small gullies and tributaries coming from the hills, West of the coring site.

3.2. Coring, and lithological description

In October 2018, a total of 39.185 m of sediment were retrieved (**Sup Fig. 1**) from six different holes in close vicinity (less than 20 m). For this survey, two Uwitec 90-mm diameter piston corers were used, the pushing power was provided using a semi-manual UWITEC downhole hammer, operated from an UWITEC platform (EDYTEM/LSCE/C2FN) acquired as part of the CLIMCOR equipment of excellence program (CNRS). This coring system was successfully applied in the Lake Iseo deep basin and permitted to overcome the challenges of deep-water coring. Sections from the different holes were taken with a 1 m shift to ensure a sufficient overlap to provide a continuous record (**Sup Fig. 1**). Most of the sections were split, photographed at high-resolution (20 pixels.mm^{-1}), described and logged in detail using the Munsell colour chart. The identification of specific layers on the overlapping sections combined with correlations of the XRF-core scanner signals allowed construction of a 15.5-m-long composite sediment sequence (hereafter called SEB18, **Sup Fig. 1**). One gap occurs in the sequence from 1342.4 to 1362.4 cm: between two sections where an overlapping section is missing. While describing the core sections, specific attention was given to the identification of layers interbedded within the continuous sedimentation. These event layers were visually documented, described, measured, and logged.

3.2. Loss on ignition (LOI)

LOI analysis was conducted to assess the organic matter and carbonate content throughout the sediment sequence. As many layers interrupt the sediment record in SEB18 section, we decided to apply a 10 cm evenly spaced discrete sampling step on the continuous sedimentation of the sediment sequence to perform LOI following the protocol that was defined by Heiri et al. (2001). Several discrete samples were also collected in the main event layers, but these data were not added in the calculation of fluxes hereafter. Before the LOI analysis, the dry bulk density (DBD) was calculated from the same sediment samples by performing a constant volume sampling and weighting the sediment after 72 h of drying at 60 °C. Then, the sediment samples were crushed before being heated in an oven at 550 °C for 4 h and at 950 °C for 2 h. The relative weight loss during the first (hereafter, LOI550) and second heating phases (hereafter, LOI950) corresponds to the fractions of organic matter and of carbonate, respectively. Finally, the non-carbonate ignition residue (NCIR) was obtained by removing LOI550 and LOI950 from the initial dry weight.

3.3. Geochemical analyses

To characterize the variations of major elements, we performed X-ray fluorescence (XRF) geochemical analyses on the EDYTEM laboratory's AVAATECH Core Scanner (Avaatech XRF Technology) throughout the SEB18 sediment sequence. We applied a continuous 5 mm step measurement with two runs: one at 10 kV and 0.3 mA for 30 s, to detect lightweight elements, such as Al, Si, K, Ca and Ti and a second run performed at 30 kV and 0.4 mA for 40 s, to detect Mn, Fe, Br, Rb, Sr and Zr. The XRF core-scanning results are expressed hereafter as count per second (cps) within each element-attributed X-ray fluorescence energy range. To identify principal sediment end-members and correlations between the detected elements, a principle component analysis (PCA) was conducted on the whole XRF dataset (Sabatier et al., 2010).

3.4 Chronology

On SEB18 sediments, we combined varve counting and ^{14}C to build a reliable age-depth model along the 15.5 m of the composite section. Varves were counted on the first 37 cm of SEB18_I_Pil02 section. Thirteen samples of terrestrial organic macroremains were used to perform ^{14}C measurements at the LMC14 laboratory (CNRS). Dates were calibrated at 2-sigma using the Intcal13 calibration curve (Reimer et al., 2013). We used the R code package “clam” (Blaauw, 2010) to compute the age-depth model of the non-event sections as this model allows to outlier some dates and to remove instantaneous event layers.

4. Results

4.1. Seismic survey

Assuming a P-wave velocity (Vp) of 1450 $m.s^{-1}$, the seismic signal penetrated 25 to 30 m of sediment below the lake floor. In areas where free gas occurs, in particular near deltas where high amount of organic matter is buried, penetration is less and characteristic high-amplitude anomalies occur that mark the gas front (**Figs. 1C & D**). The seismic facies comprise sections where seismic reflectivity is high and subparallel reflections with high lateral continuity occur; these are interpreted as regularly stacked continuous sedimentation. The associated reflections all onlap the steep lateral sides of the lake basin. Intercalated within these reflective sections, several transparent to chaotic deposits typical of mass-wasting deposits (MWD) (e.g. Chapron et al., 2016; Strasser et al., 2013) interrupt the continuous sedimentation. They often show high amplitude reflections at their bases. The upper part of these MWDs is usually transparent, indicating a megaturbidite/homogenite unit representing the latest stage of event sedimentation when the fine particles eventually settle. The lower parts of MWDs may show some internal architecture with reflections indicating various basal flow units. Some of the MWDs show a mound-like geometry with larger thickness in the center of the basin (**Fig. 1D**). At least, eight MWDs are identifiable across the deep basin of Lake Iseo, with three deposits presenting a metric thickness (**Fig. 1C & D**). Most of these deposits seem to cover the entire basin, and, considering their geometry, to originate from its Southern or Northern part. MWD1 is identified at the base of the Western slope of Monte Isola and laterally evolved towards the deep basin into transparent acoustic facies (**Fig. 1C & D**).

The three thickest MWDs are labelled MWD1, 2 and 3 (**Fig. 1C, D & Fig. 2**). Interpolation of their thicknesses result in volume estimates of $11{\cdot}10^6$ m^3 for MWD3 and a combined $89{\cdot}10^6$ m^3 volume calculated for both MWD1 and MWD2 as they are stacked and partly hard to be subdivided on the seismic data.

4.2. Sedimentology

4.2.1 Lithologies and stratigraphic units

Along the 15.5 m of the SEB18 sediment sequence, laminated sediments, interpreted as Lake Iseo continuous sedimentation, occur in 39 % of the sedimentary succession. They are clearly distinguishable from homogeneous or graded layers, which are thus interpreted as event layers and account for 61 % of the total accumulation. Within the continuous sedimentation, two stratigraphic units can be distinguished (**Fig. 2**): Unit I (0 – 32.3 cm) is composed of dark grey clay becoming greenish at the base of the unit. It is composed of thin alternations of light greyish olive clayey (10Y 6/2), grey (5y 5/1), pale yellow (5Y 7/3) and dark laminae (5Y 2.5/1). Fifty-eight laminae successions were counted in this unit that also includes several graded layers. This unit coincides with the varved organic gyttja which has already been described in cores retrieved in Lake Iseo (Lauterbach et al., 2012; Rapuc et al., 2019) and related to the recent eutrophication period of Lake Iseo. No analyses of LOI were conducted on this unit.

In Unit II, from 32.3 cm to the bottom of the core (1550.9 cm), the continuous sedimentation of the SEB18 sedimentary section is composed of grey clay (10YR 5/1) rich in dark mineral that disappear after oxidation. The LOI550 ranges between 3.8 and 7.5 %, with a mean value of 5.3 %. The LOI950 ranges between 5.7 and 18.2 % with a mean value of 12.2 %. This corresponds roughly to ca. 15 to 45 % of carbonates, which is low compared to a similar lake, such as Lake Bourget (40 to 80 % $CaCO_3$), over the same time-period. The continuous background sedimentation of Unit II is interrupted by many graded layers described below. The grain-size of the continuous sedimentation is largely dominated by fine silts and clays (Q90 < 20 µm).

4.2.2. Event layers

The SEB18 sediment section presents several layers that are clearly distinguishable from the continuous sedimentation by their colours and textures. These graded layers were identified and counted macroscopically. Their colours vary from dark grey to light brown (2.5Y 5/2), very dark greyish brown (10YR 3/2), dark grey (10YR 4/1) and black (10YR 2/1). These layers either have a normally-graded upward-fining grain-size pattern like turbidite type deposits or they display homogeneous lithologies termed “homogenites” (Hieke, 1984; Kastens and Cita, 1981). As they interrupt the continuous sedimentation, they are considered as instantaneous event layers. The thickest layers present fine to medium sand at their bases (Q90 > 200 µm). Most of the layers are thin (i.e. below 1 cm), but three of them are complex sequences that reach thicknesses higher than 1 m : (i) Event layer 1 (EL1) is comprised between 1178.5 and 1320.7 cm, (ii) Event layer 2 (EL2) is 3.37 m thick and located between 682.3 and 1020 cm and, (iii) Event layer 3 (EL3) is comprised between 493.5 and 626.1 cm in the SEB18 sediment sequence (**Fig. 2**). EL1 and EL3 present a fine graded sandy base followed by a thick homogeneous part, composed of very fine sand to silt and a thin dark clayey top. EL2 is the thickest layer in SEB18 sediment sequence. It presents a lower part composed of medium to fine sand associated with mud-clasts probably remobilized upstream of the coring site due to erosive turbid flows. This is followed by homogeneous silt from 891. 5 cm to 683.7 cm and a thin clayey top. EL1, 2 and 3, such as most of layers thicker than 5 cm, present an erosive base. They are also identifiable on the seismic profiles (**Fig. 1C, D & Fig. 2**) as they are correlated to MWD1, 2 and 3, respectively, and seem to originate from the Oglio delta in the Northern part of the deep basin and at times from the Southern part. The event layers equal to or thicker than 1 mm were identified and counted resulting in a total of 146 layers throughout the SEB18 sediment sequence. Their average thickness is 6.5 cm and the median is 1.2 cm.

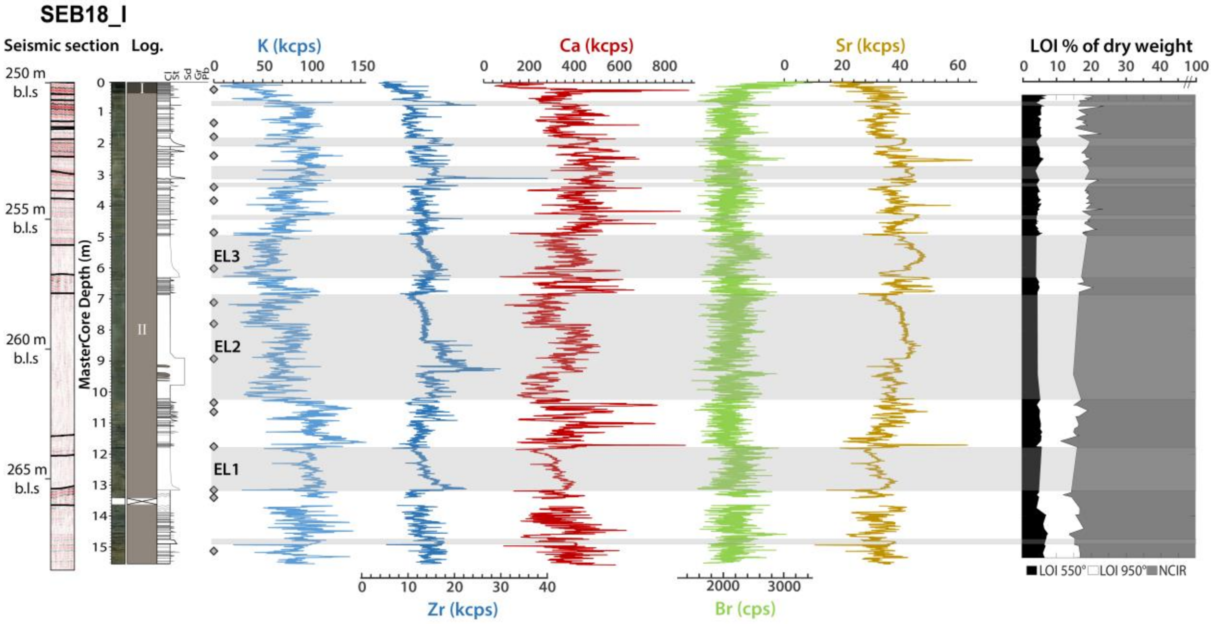

*Figure 2 -Sedimentological and geochemical data. A close-up view of the seismic profile (**Fig. 1C**) section is compared with lithological and geochemical data. A core image of the 15.5 m of the SEB18 sediment sequence and stratigraphic units are associated with the grain-size sensitive lithological column, selected geochemical results (K, Zr, Ca, Br, and Sr contents) and LOI. The depth of the seismic section is expressed in metres below lake surface using a Vp of 1450 $m.s^{-1}$ and is scaled approximately to fit the length of the sediment core. Grey shadings represent the thickest graded layers. Grey diamonds represent junction between the different sections of SEB18 sediment sequence.*

4.2.3. Geochemical analyses

Unit I shows low values of K (< 70,000 cps), of Zr (< 10,000 with only one peak at 15,000 cps) and an upward increase of the Br values to the top of the unit (from 2000 to 3000 cps). In the continuous sedimentation, the Zr and K signals increase downcore (**Fig. 2**) toward the base of the sediment sequence (Unit 2). No clear trend is visible for other elements, as Ca, Br and Sr display relatively constant values in the background sediments. Graded layers are not always clearly distinguishable from the continuous sedimentation using XRF data. Most event layers are however characterized by a peak of Zr at the base and an increase of K value towards the top (**Fig. 2**). Br and Ca are very variable and fluctuate within the event layers, while Sr shows low variability. Few samples were collected in these thickest event layers and do not present significant changes in the LOI550 and LOI950 values. Individual and variables factor maps were obtained from a PCA conducted on the XRF data (**Fig. 3**).

These figures highlight the geochemical distribution within the two different sedimentary units and the relationships between the different elements. Dimensions 1 and 2 (denoted as Dim1 and Dim2) represent 52.7 % of the total variability. Three chemical end-members were identified from the variables factor map. The first one is positively correlated with Dim1, yields high positive loadings for the major terrigenous elements (Al, Si, K, Ti, Rb, Fe), and is thus denoted as “terrigenous”. The second end-member, shows negative loadings on Dim2 and allows the discrimination of Br, Mn and Pb. Br was previously correlated in other cores of the same lake to organic matter content and Mn to oxygenation processes in the lake (Rapuc et al., 2019), Pb is probably complexed with organic matter. This pole is then denoted as “organic matter”. The third end-member, shows positive correlation with Dim2 and yields high positive values for Zr, Ca and Sr. Sr is usually present in marine limestone, which constitutes a major part of the watershed's outcrops. Zr is generally associated with coarse grain-size explaining the peak at the base of each thick coarse graded layers. Thus, this end-member is interpreted as representative of the carbonates and coarsest terrigenous inputs from the watershed, characterised by the presence of reworked marine carbonates (Ca, Sr) and heavy minerals (Zr). It is thus denoted as “coarse terrigenous fraction”.

To understand the specificity of the two stratigraphic units and the different event layers, an individual factor map was drawn (**Fig. 3B**). From this map, Unit I is negatively correlated with terrigenous end-member and positively with the organic matter end-member. This confirms its dominant organic content already observed in other cores from Lake Iseo (Lauterbach et al., 2012; Rapuc et al., 2019). Unit II presents a large variability but is in general positively correlated with the terrigenous end-member and is also characterized by low Ca, Zr and Sr counts. The event layers present a wide distribution on the individual factor map, and are characterised by relative low organic matter content. PCA analyses from XRF data did not allow to classify event layers in different types.

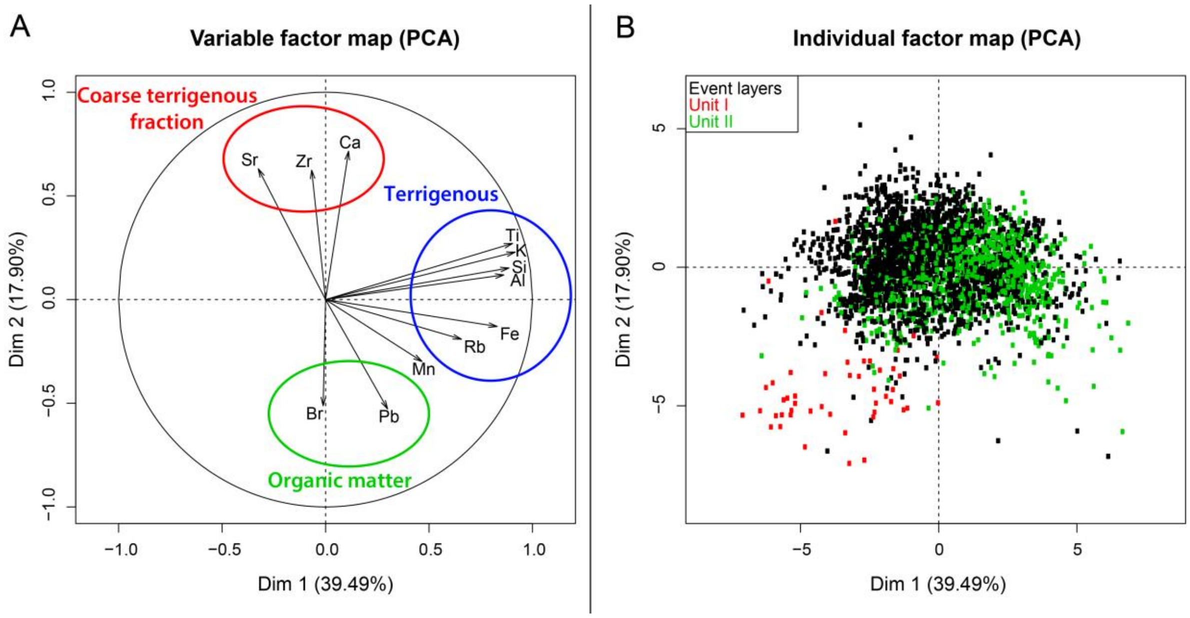

Figure 3 - Variable and individual factor maps from the PCA. (A) Variable factor map with three end-members (terrigenous, organic matter and carbonates). (B) Individual factor map with the two sedimentological units added as an illustrative variable and compared with the event layers.

4.3. Chronology

From the first 37 cm, 58 varve couplets were identified and counted, yielding a mean sedimentation rate of 5.3 $mm.yr^{-1}$ once the thickness of the detrital events was removed. This counting allows to assign the earliest varve to 1960 CE corresponding to the beginning of the eutrophication of the Monte Isola Plateau, already established by varve counting from the SEB10 sediment sequence (Rapuc et al., 2019). This timing is quite identical to the one observed in Lake Varese, in Northern Italy (Bruel et al., 2018) where both climatic and anthropogenic impacts are supposed to have influenced lake anoxia. The uppermost turbidite is assigned to 1994 CE and corresponds to a well-documented flood event (Guzzetti and Tonelli, 2004; Luino et al., 2002).This turbidite was used as chronological marker included in the age-depth model.

Thirteen samples of terrestrial macro-remains were analysed to provide radiocarbon ages. Once calibrated, 4 of these 13 dates (**Table 1**) were not used because they presented ages older than the best-fit age-depth curve of the SEB18 sequence. All these four ages were sampled from the top of graded detrital layers, so that these macro-remains are interpreted as reworked from previously deposited sediment in the lake.

Table 1 - Radiocarbon ages for the SEB18 sediment sequence. Event free depth was calculated by excluding the thicknesses of each graded beds that were considered as event layers. Samples in bold correspond to dates excluded from the age-depth model (Fig 4, B and C).

Sample name	Core	Depth (cm)	Event-free depth (cm)	Radiocarbon age	Age cal yr BP 2 σ range	Type
SAC-A 57155	SEB18_I_C_01A	169.8	120.8	170±30	-3-289	stem
SAC-A 57512	**SEB18_I_B_02A**	**271.8**	**179.3**	**465±30**	**490-538**	**plant debris**
SAC-A 57513	SEB18_I_C_02A	395	229.3	555±30	520-639	plant debris
SAC-A 57156	SEB18_I_B_03A	463.7	270.4	745±30	662-726	plant debris
SAC-A 57514	**SEB18_I_C_03A**	**488.2**	**294**	**1015±30**	**802-978**	**plant debris**
SAC-A 57157	SEB18_I_B_04A	653.2	314.7	950±30	796-925	plant debris
SAC-A 57515	**SEB18_I_C_04A**	**702.9**	**324.9**	**1190±30**	**1007-1226**	**wooden debris**
SAC-A 57516	SEB18_I_B_06A	1058.7	340.2	1000±30	799-966	plant debris
SAC-A 57158	SEB18_I_C_06A	1136.4	385.4	1150±30	980-1173	plant debris
SAC-A 57517	SEB18_I_C_06A	1153.4	400.5	1255±30	1085-1277	plant debris
SAC-A 57518	**SEB18_I_B_07A**	**1183.4**	**420.2**	**1575±30**	**1401-1535**	**twig**
SAC-A 57519	SEB18_I_B_08A	1406.9	502.8	1550±30	1379-1526	plant debris
SAC-A 57520	SEB18_I_B_08B	1548.9	598.7	1980±30	1876-1992	plant debris

All the event layers identified and counted previously were interpreted as instantaneous events. The thickness of each layer was thus subtracted from the SEB18 sediment sequence depth to create an event-free depth (**Fig. 4A**) in order to obtain the best age-depth model (Wilhelm et al., 2012). We use the combination of varve counting and the nine remaining calibrated ages to generate the age depth-model using the R code package "clam" (Blaauw, 2010) with a smooth spline model with 0.4 for the smooth parameter. The sedimentation rate presented hereafter (**Fig. 4B**) was calculated from the event-free depth and is not influenced by the variation of the event layer occurrences. To provide a date for all event layers, we reintegrated all event layers to the age-depth model (**Fig. 4C**).

The first 15.5 m of sediment retrieved in the deep basin of Lake Iseo on SEB18 coring site covers the last 2000 yrs with a continuous sedimentation rate (without event layers) that varies between 5.1 and 2.1 mm.yr^{-1} with a mean of 3.1 mm.yr^{-1}. No hiatus was identified. The sediment sequence thus covers the period between 2018 and 21 CE. Two peaks and a period of gradual increase of sedimentation rate are identified (**Fig. 4B**) in the sequence. The first peak occurs at ≈ 660 CE with a sedimentation rate of 3.15 mm.yr^{-1}. After a decrease until 891 CE (2.72 mm.yr^{-1}), the sedimentation rate increases gradually until a maximum of 3.06 mm.yr^{-1} at ≈ 1360 ± 49 CE that precedes another small decrease until 1520 ± 69 CE with a sedimentation rate of 2.86 mm.yr^{-1}. From then towards the top, the sedimentation rate increases sharply and reaches its highest value of 5.05 mm.yr^{-1}

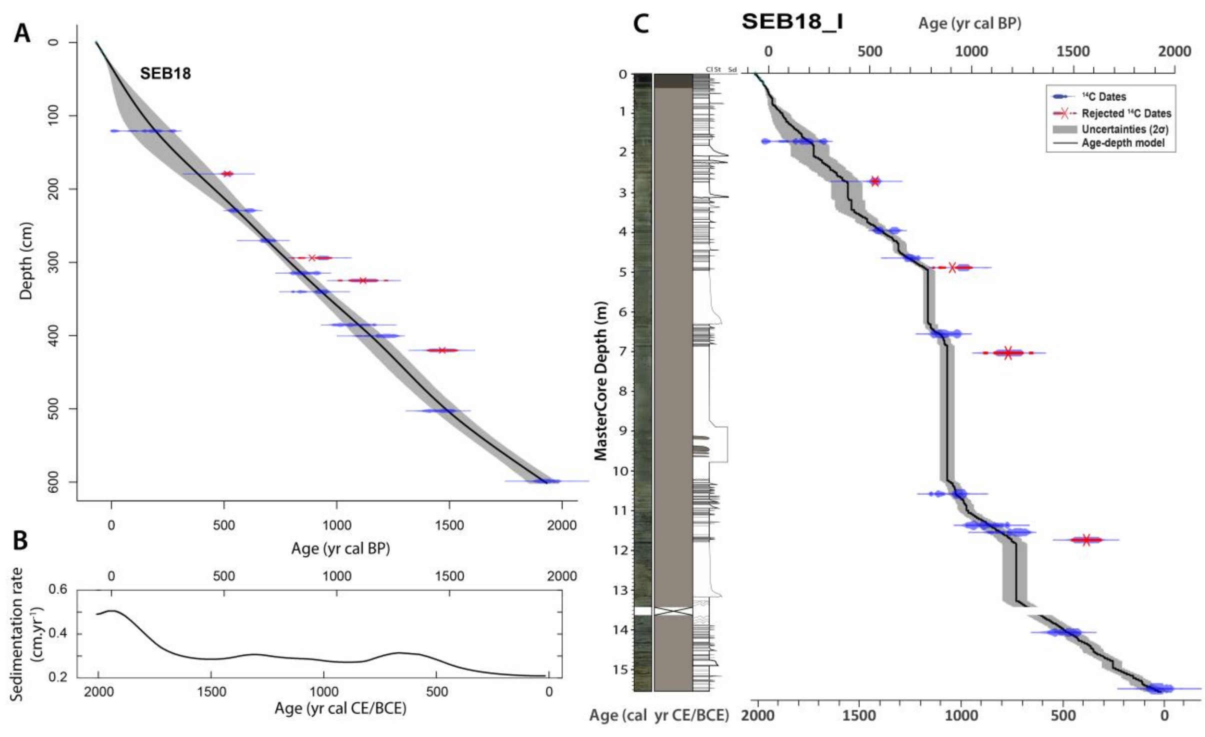

Figure 4 -Age-depth models. (A) Age–depth model in event-free depth. (B) Sedimentation rate (without event layers) obtained from the age-depth model, (C) Complete age-depth model associating radiocarbon and varve counting.

5. Interpretation and discussion

5.1. Origin of continuous sedimentation

The mean sedimentation rate (without event layers) measured in the SEB18 sequence is above 3 $mm.yr^{-1}$. LOI analyses indicate that organic matter accounts for only 5.3 % of the main sedimentation, and biogenic and detrital carbonates represent only 12.2 %. Thus, most of this sedimentation corresponds to siliciclastic input into the lake (82.5 %). Lake Iseo is a meromictic lake, where the deep water does not mix every year. The ARPA instrumental data (Regional Agency for the Protection of the Environment, http://arpalombardia.it/) indicates that pH values decrease sharply between 80 and 100 m b.l.s at the upper limit of the hypolimnion (**Fig. 5A**). This variation is accompanied by an increase in dissolved calcium concentration (**Fig. 5B**). Depending on the particle sizes and the settling times, redissolution of carbonates can occur at great depth in hard water lakes (Ramisch et al., 1999). For instance, in Lake Lugano, a peri-alpine lake with a maximum depth of 288 m, only particles with a diameter larger than 40 µm reach the lake bottom (Ramisch et al., 1999). Yet, authigenic carbonates have a low sinking velocity and present usually a diameter lower than 20 µm, such in Lake Bourget (Arnaud, 2005). Then, authigenic carbonates are not likely to be preserved during their settling in the deep basin of Lake Iseo and are not supposed to contribute significantly to the continuous sedimentation. Then, thin authigenic biogenic carbonates can only be preserved above a certain depth, where redissolution processes do not impact small size particles. In Lake Iseo, these particles can thus only accumulate above the hypolimnion on slopes and plateau (**Fig. 5C & D**) presenting an inclination lower than the theoretical angle of repose of wet clayey material (> 30°, Glover, 1997). Thus, in the deep basin, as settling times plays an important role, most of the carbonates recorded in the continuous sedimentation are supposed to be linked to detrital inputs from the watershed through erosion of the limestone and marlstone bedrock, which is strongly suggested by the correlation between Ca, Sr and Zr.

The SEB18 coring site is located ≈ 11 km away from the inlet of the Oglio river, the main tributary of the lake. Oglio river waters and thus the sediment inflow by the Oglio plume are deflected towards the Western shore of Lake Iseo due to the Coriolis influence (Pilotti et al., 2018, 2013). In normal conditions, the water underflow coming from the Oglio inlet only influences the first 100 m of the lake basin, while the horizontal length of overflow intrusion is supposed to be limited to 3 km (Hogg et al., 2013). Thus, most of sediment input from the Oglio river during normal flow conditions is accumulated close to the delta or on the North-Western shores of Lake Iseo. Therefore, the input of detrital sediment in the deep basin can be mainly related to flood events : when the current is strong enough, underflows can flow beyond the delta and lead to the settling of thin particles after the decrease of the turbiditic current in the deep basin. It is thus very likely that the continuous detrital sedimentation of the deep basin of Lake Iseo corresponds to the decantation of the end of underflows linked to low return period flood events. A minority of this sedimentation can also be linked to gullies and small rivers from the hillslopes West and East of the deep basin. However, SEB18 coring site is protected from underflows coming from all the inlets located in the Marone delta or feeding Monte Isola Plateau and the Sale Marasino Basin by the presence of the ridge North-West of Monte Isola (**Fig. 1B**).

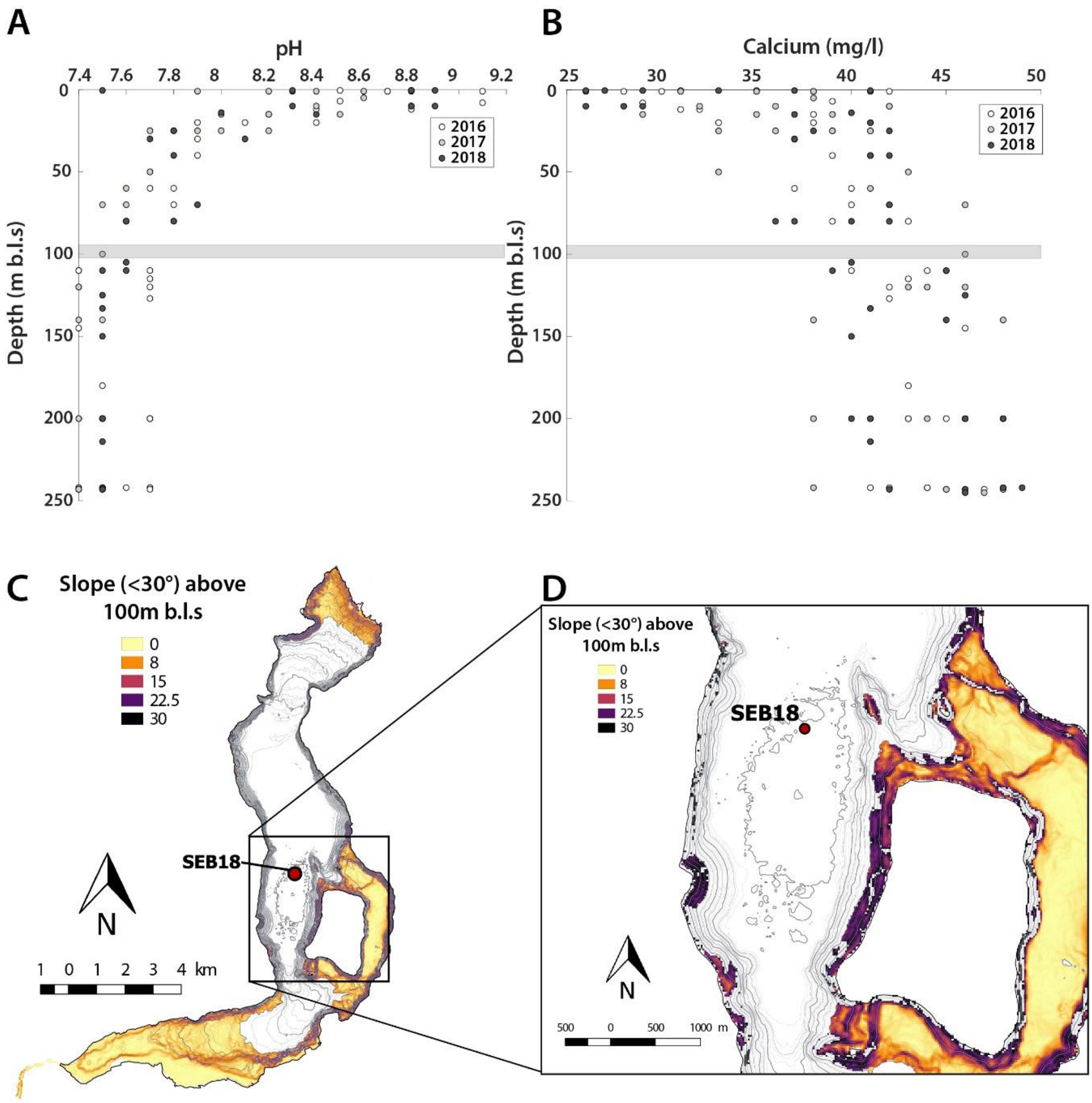

Figure 5 – Ph (A) and dissolved calcium (B) profiles, recorded in the deep basin of Lake Iseo, close to the coring site, in 2016, 2017 and 2018 by ARPA (http://arpalombardia.it/). (C) Map presenting slopes of Lake Iseo with an inclination lower than 30° above 100 m b.l.s. where authigenic carbonates could accumulate (D) Zoom of map C in the deep basin around the coring site.

5.2. Origin and trigger of the event layers

In large lowland lake systems, several mechanisms can trigger event layers, such as : (i) considerable lake-level fluctuations, (ii) destabilisation of slopes and deltas due to sediment overloading or (iii) to seismic shaking and, (iv) flood events (e.g. Rapuc et al., 2018; Sauerbrey et al., 2013). Here, we found no evidence of significant fluctuations of the lake level, thus, this triggering mechanism cannot be invoked to explain thick layers recorded in the deep basin. Due to the high sedimentation rate recorded over the last 2000 yrs in the deep basin (**Fig. 4B**), sediment overloading on the lake slopes, on the delta of the Oglio, or on those of small tributaries are likely to induce slides leading to the deposition of graded layers in the deep basin of Lake Iseo. Equally, this high sedimentation rate implies a high sensitivity of the lake to seismic shaking (Rapuc et al., 2018; Wilhelm et al., 2016). With a mean sedimentation rate of 3.06 $mm.yr^{-1}$, the probability for an earthquake to induce a slide and related event layers in Lake Iseo is higher than in most of previously studied Alpine lakes (Wilhelm et al., 2016). Moreover, such lake basins with sharp shelves and a flat lake floor provide typical settings for mass movements (Sauerbrey et al., 2013). In terms of flooding, as previously mentioned, most of floods contribute to the continuous background sedimentation in the deep basin of Lake Iseo with the distal low-velocity underflows reaching the coring site with the finest suspended particles. In contrast to these signatures of floods in the background sediments, floods can be recorded in the deep basin as event layers either when (i) strong underflows linked to extreme flood events produce a current important enough to reach the deep basin and produce a turbidite layer distinguishable from the continuous sedimentation as for the 1994 CE event, or when (ii) flood events come from nearby tributary rivers. In summary, only three mechanisms can be at the origin of the event layers recorded in the SEB18 sequence: (i) sediment overloading on slopes or deltas producing spontaneous mass movements, (ii) extremes floods events from the Oglio river or floods events from gullies and small tributaries coming from the Western hillsides of the lake, and (iii) destabilisations of slopes and delta triggered by seismic shaking.

In the SEB18 sequence, 146 graded layers were identified and interpreted as event layers. Colours and textures from macroscopic observations, XRF data and PCA were insufficient to distinguish and classify these layers and to link them to a specific triggering mechanism. This is probably due to the high variability of XRF signals within each layer or due to the multiple provenances of sediment particles in the deep basin of Lake Iseo. Large lakes are characterized by multiple rivers or gully inlets and a large diversity of sediment facies accumulated from the top to the bottom of the slopes depending on the location and the depth. This variety of sources makes it difficult to study the origin of event layers in a large lake. Only a thorough knowledge of the functioning of the sedimentation in the lake, associated with a multiproxy approach, can help to disentangle the different origins of the sediment in event layers and allows the interpretation of their triggering mechanisms. To do so, we had to identify the potential source areas and transport mechanisms of each event layer.

5.2.1. Locating potential source areas

We assumed there could be only two potential sources of sediment making the event layers: (i) detrital sediment from the Oglio delta and (ii) sediment from lake slopes overhanging SEB18 coring site (lateral sources). To distinguish those source areas, we had to consider together the chemical composition and the thickness of the event layers.

Indeed, whereas deltas are obvious sources of event layer, through stream flood and delta collapse, any sediment accumulation overhanging SEB18 coring site could potentially slide down to the lake bottom, provided that it is thick enough. Such a thick accumulation may not occur on slopes > 30° in the absence of progradation process. Moreover, in the absence of major terrigenous input such accumulation should be made of in-lake produced biogenic compounds. If such a source exists it hence requires to present slope < 30° and be favourable for biogenic matter accumulation, which in hard-water lakes is mainly made of calcite. However, it has been shown that the preservation of biogenic calcite in lakes drastically decreases with depth, depending on carbonate particle size. In the case of Lake Iseo, water chemistry indicates the reach of a steady state in [Ca+] around 100m (**Fig. 5**), suggesting that at this depth, most of the biogenic calcites settling from the surface has been dissolved. This is consistent with what has been observed and modelled in Lake Lugano (Ramisch et al., 1999) which presents a similar setting. One may thus assume that, if lateral sources of event layers exist, they should be located on < 30° and < 100 m deep slopes overhanging SEB18. **Fig. 5C & D** shows the distribution of such areas.

5.2.2. Chemical distinction between delta and lateral sources

Distinguishing those sources basically consists in distinguishing sediments rich in biogenic vs. terrigenous carbonate. As lake waters are depleted in Sr compared to marine waters (e.g. Brown and Severin, 2009 and references therein; Faure et al., 1967), lacustrine biogenic carbonates present a Ca/Sr ratio higher than marine carbonates that are part of the lake watershed (Faure et al., 1967). Thus, the Ca/Sr ratio can be used as a proxy to distinguish sediment with a detrital input (low Ca/Sr value) from sediment more influenced by in-lake biogenic carbonate precipitation (with a higher Ca/Sr value). As the continuous sedimentation is composed by no or very few biogenic carbonates, in relation to carbonate dissolution in the water column (**Fig. 5**), the mean Ca/Sr value of an event layer (Ca/Sr_{mean}) with a detrital origin is supposed to be equal or lower than the mean Ca/Sr value of the continuous sedimentation (Ca/Sr_{consed}). On the contrary, event layers with a $Ca/Sr_{mean} > Ca/Sr_{consed}$ are interpreted as relatively enriched in lacustrine biogenic carbonate and thus deriving from lateral sources (**Fig. 6A**).

5.2.3. Distinguishing flood- and mass wasting- deposits originating from the delta

If we are able to distinguish lateral from delta sediment sources, it remains uncertain whether an event layer coming from the delta was triggered by a flood or by a delta collapse. The relationship between the maximum grain-size and the thickness of event layers may here be useful to discriminate the transport processes leading to their deposition (**Fig. 6B,** Wilhelm et al., 2013). Indeed, due the distal position of SEB18 relative to the Oglio delta, only massive delta collapse-associated deposits may reach it, at the inverse of flood-triggered underflows which may run over long distance on the bottom of the lake. Moreover, slides and slumps are generally more sediment-loaded than flood-triggered underflows. Consequently, their mean grain-size is lower than those of underflow deposits due to a more important dilution of coarse particles by the clayey matrix that supports the sediment transport.

Hence, we may assume that, for a given grain-size, a mass wasting deposit will be much thicker than a flood-triggered deposit (Wilhelm et al., 2013).

To assess the grain-size of each of the 146 event layers, we use the maximum value of Zr/K ratio, a commonly-used chemical proxy of grain-size (Cuven et al., 2011, Sabatier et al., 2017, Rapuc et al., 2019; Wilhelm et al., 2013). Indeed, Zr is interpreted as a proxy of heavy minerals, while K is linked to fine-grained particles such as clay (Cuven et al., 2010; Kylander et al., 2011). In **Fig. 6B**, the limit of 40 mm allows to distinguish two groups of event layers. A thin layer (< 40 mm, **Fig. 6B**) with a high Zr/K_{max} value is composed of coarse grains with a low volume of transported sediment. Such a layer requires strong water currents, as turbiditic currents during floods and resulting underflows (Sturm and Matter, 1978). Event layers linked to a slide or a slump of previously deposited sediments are not linked to water flow and thus present a lower grain-size for a similar thickness (Wilhelm et al., 2013). Layers presenting a low Zr/K_{max} associated with an important thickness (> 40 mm) thus correspond to slide or slumps from slopes or deltas.

5.2.4. Attributing triggering mechanism to event layers

The combination of Ca/Sr_{mean} as a proxy of the sediments source, with Zr/K_{max} and the thickness of each event layer as proxies of transport processes, allows to distinguish and interpret the origin among the three different types of layers (**Fig. 6**). Type 1 regroups thin layers (< 40 mm) presenting a high Zr/K_{max} and a low Ca/Sr_{mean} value (**Fig. 6**). These layers are interpreted as composed of detrital sediment transported by an underflow. Underflows that reach the deep basin of Lake Iseo can only be linked to extreme flood events from the Oglio river or from the small hillslopes' tributaries. Type 1 regroups 41 layers that represent a total thickness of 42 cm. Twenty-one layers, accounting for a thickness of 28 cm present low Zr/K_{max} and low Ca/Sr values, reflecting thin detrital inputs or inputs depleted in biogenic carbonates. These layers, labelled as Type 2 layers, are uninterpreted because they can be linked to (i) flood from small tributaries associated with a weak current that does not transport coarse grains or (ii) slides from slopes depleted in biogenic carbonates, namely, located in the hypolimnion (below 100 m b.l.s.) were biogenic production is poorly preserved due to low oxygen concentration and pH (**Fig. 5**). Type 3 regroups (i) layers presenting high Ca/Sr_{mean} and low Zr/K_{max} values that are composed of sediment enriched in biogenic carbonates coming from smooth slopes above 100 m b.l.s around the core site (**Fig. 5D**) and (ii) thick layers (> 40 mm) composed of detrital materials (low Ca/Sr) that originates from the Oglio delta or smaller tributaries deltas. The relationship between the thickness and the Zr/K_{max} of this last group corresponds to a slide or slump-like transport (**Fig. 6B**). Type 3 layers regroup all layers composed of sediment previously deposited in the lake and remobilized after sediment overloading or seismic shaking. Of the 146 layers and the 9.52 m of sediment thickness for event layers, 84 correspond to Type 3 layers and represent 8.81 m of sediment in the SEB18 sequence. Fifteen layers show a detrital origin, and the other 69 layers are enriched in biogenic carbonate and thus originated from slopes above 100 m b.l.s. This result is coherent with the high sensitivity of Lake Iseo to record seismic activity due to its high sedimentation rate.

To strengthen the interpretation of the different origins of event layer types, we compare the ages of several events with the Italian historical seismic catalogue (CPTI15, Rovida et al., 2020, 2019) and local documented flood events (Guzzetti and Tonelli, 2004; Luino et al., 2002). The three thickest Type 3 layers (EL1, EL2 and EL3), observed on seismic profiles (**Fig. 1C & D**) present a detrital signature and are supposed to be triggered by the remobilization of detrital sediment from the Oglio delta during earthquakes. Indeed, the Oglio delta is several kilometres long and is the principal source that can produce 1.3 to 3.4 m thick detrital layers covering the centre of the deep basin and representing a total of ≈ 100 km^3 of sediment deposited. EL3 (11 km^3), is dated between 1120 and 1220 cal CE; considering ^{14}C dating uncertainties, it can be correlated to the 1222 CE earthquake that caused heavy damage in the Brescia area (less than 30 km distance from the lake). Despite the fact that the earthquake source cannot be unquestionably identified from both geological surveys (e.g. Livio et al., 2009) and macroseismic data (Guidoboni et al., 2005); the earthquake parameters are largely imprecise (see a comparison of epicentral location, and derived magnitude at https://emidius.mi.ingv.it/ASMI/event/12221225_1230_000), the historical chronicle refer to repeated events, and damages that are compatible with low frequency, long duration shakings. This seismic event was also identified in Lake Iseo sub-basin (SEB05 & 06 sequences; Lauterbach et al., 2012) and in Lake Como (**Fig. 1**, Fanetti et al., 2008) where it has been associated to a ≈ 3 km^3 megaturbidite deposit. The thickest detrital Type 3 layer, EL2, is dated between 1020 and 1125 cal CE and can be tentatively correlated to the 1117 CE earthquake: this event is one of the strongest and most damaging historical earthquakes documented in Northern Italy (Galadini et al., 2001; Gasperini et al., 2004). It occurred probably South of Verona (about 80 km distance, South-Eastward of Lake Iseo) with damage of intensity VII MCS both in Brescia and Milan; the expected shakings in the lake area should have been therefore similar to the one caused by the 1222 earthquake. Alternatively, this layer can be associated also to the 1065 CE Brescia earthquake, for which only two macroseismic observations (Brescia, VIII; Milan, Felt) are available, and the level of ground motion at Lake Iseo is highly speculative. Moreover, the continuous sedimentation intercalated between these two thick event layers represents around 93 years, which, considering that the base of EL2 is erosive, almost corresponds to the gap between the two historical seismic events. The oldest thick detrital Type 3 layer, EL1, is dated between 640 and 830 cal CE. For this event there is no earthquake in the Italian historical macroseismic archive (https://emidius.mi.ingv.it/ASMI/) that can be reasonably associated to the layer, but it is known that in Middle Ages the database is incomplete, also for major events. The nearest earthquake in time and space is the one referred to Treviso in 778 CE, but the expected ground motion at Lake Iseo due to this earthquake, cannot be responsible for massive slope instabilities. Another megaturbidite that led to a ≈ 10.5 km^3 sediment deposit resulting from large slides from steep slopes was recorded in Lake Como and might coincide with another megaturbidite deposit in Lake Sils dated at ≈ 700 cal CE (Blass et al., 2005).

Concerning Type 1 layers, some of the most recent layers present the same ages as local and regional historical flood events such as the 1991, 1960, 1952 floods that impacted the city of Darfo Boario Terme (Luino et al., 2002) or the 1994 regional flood event that impacted the Po Plain (Guzzetti and Tonelli, 2004).

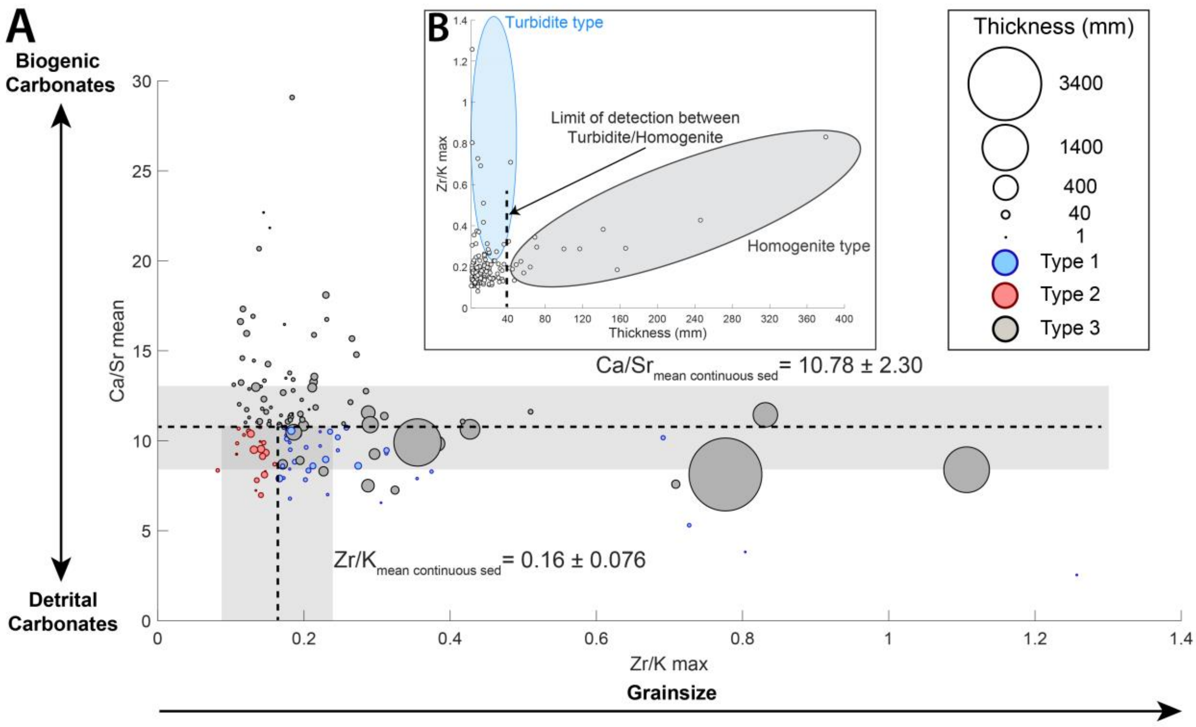

Figure 6 – (A) Scatter plot of Ca/Sr$_{mean}$ versus Zr/K$_{max}$ with the thickness indicate by dot sizes of each event layers. (B) Scatter plot of Zr/K$_{max}$ values versus the thickness of each event layers.

5.3. Link between sediment inputs and the frequency of sediment remobilisation

A siliciclastic terrigenous flux (SCTF; g.cm^{-2}.yr^{-1}) was calculated to characterize the evolution of erosion processes in Lake Iseo catchment (**Fig. 7A**). SCTF was computed as the product of the % of non-carbonate ignition residue (NCIR) by the sedimentation rate (without events) and by the sediment DBD (Rapuc et al., 2019). The SCTF could be interpreted as the evolution of total terrigenous flux in the deep basin of Lake Iseo and used as a proxy of erosion (Bajard et al., 2017). However, Type 1 layers were interpreted as flood events and thus correspond to detrital input from the watershed. We computed another SCTF using the sedimentation rate calculated by adding flood layers thicknesses as suggested by Bajard et al., (2019). As Type 2 layers correspond to undifferentiated layers, that can potentially be linked to detrital input, we calculated a third SCTF including Type 1 and Type 2 layers thicknesses to test a possible influence of one or the other type of layers on the detrital flux in the deep basin of Lake Iseo. We also calculated the sedimentation rate with Type 1 and with both Type 1 & 2 layers thicknesses (**Fig. 7B**). There are very few differences between the three SCTF and the calculated sedimentation rates. However, between 800 and 1400 AD, SCTF and sedimentation rate including flood layers indicate a higher input of detrital sediment. To discuss the influence of detrital input on the frequency of remobilisation of previously deposited sediment in Lake Iseo, we will refer hereafter to the SCTF and the sedimentation rate calculated with Type 1 layers thicknesses. The frequency of Type 1 layers, interpreted as flood events, are presented as variation of the number of floods that were recorded in the SEB18 sedimentary sequence per 101 years (**Fig. 7C**). The frequency of the number of Type 3 layers per 101 years was also calculated and represents the variation of the frequency of remobilisation of sediment from the slopes and deltas (**Fig. 7D**). Due to the method of representation of the frequencies per 101 years, the sediment gap in the SEB18 sequence between 587 CE and 671 CE impacts the frequencies between 487 and 771 CE presented hereafter and on **Fig. 7C & D**. Interpretation of fluctuations of these frequencies in this period should be taken with caution. Flood and remobilisation frequencies are low at the beginning of the Roman Period with a small increase of the number of remobilisation events. Between 500 and 750 cal CE, sedimentation rate and SCTF present a first peak directly followed, from 700 cal CE, by a sharp increase of the frequency of the remobilisation of sediment in Lake Iseo. This could be explained by a long period of accumulation of sediment on slopes and on the Oglio delta that led to an increase of the sensibility of the lake to record seismic shaking. At 732 ± 62 cal CE, the first thick remobilisation event from the Oglio delta occurred (**Fig. 7E**), no other detrital Type 3 layer is recorded after this event until around 980 cal CE. The frequency of remobilisation events continues to increase until around 1050 cal CE and the occurrence of the second thickest layer (**Fig. 7F**) from the Oglio delta. The 1117 CE earthquake, producing a 3.4 m thick layer, remobilised an important volume of previously deposited sediments, causing a decrease of the amount of sediment available on the delta and on slopes for the following events and thus a decrease of the sensitivity of Lake Iseo to record following seismic shaking or slides from overloaded slopes. This event can thus explain the first decrease of the remobilisation frequency. It is directly followed by a second sharp decrease after the 1222 CE earthquake that led to the youngest thick detrital Type 3 layer. Five other periods of increase of the remobilisation frequency are observed: 1250 – 1370, 1490 – 1600, 1670 – 1790 and after 1880 cal CE (**Fig. 7D**).

The occurrence of event layers linked to a remobilisation of previously deposited sediment in the deep basin of Lake Iseo appears during or just after periods of high sedimentation rate or terrigenous input. These detrital inputs increase the load of sediment on the Oglio delta and on the lake slopes, increasing the sensitivity of the lake to record earthquake. After a large amount of sediment is remobilised and transferred to the deep basin, the frequency of remobilisation events decreases, which strengthens the link between sediment availability and frequency of remobilisation events. This is especially true regarding Type 3 layers coming from the Oglio delta (**Fig. 7E**). Moreover, it is well-established on faults in Central Italy, especially in the Apennine, that periods of high seismic activities last several hundred years and are spaced by long quiescence periods (e.g. Benedetti et al., 2013; Verdecchia et al., 2018) : implying that there is no evidence of short-term fluctuations of the seismic activity in the Italian regions that can explain changes equivalent to those observed on the Type 3 layers frequency.

A first period of flood frequency increase (Type 1) is recorded from 380 to 587 CE and is associated to an increase in frequency of Type 3 layers. From 930 cal CE and particularly after the 1117 CE earthquake, the frequency of flood events recorded in the deep basin of Lake Iseo increases sharply. This increase appears during an increase of the sedimentation rate and is interpreted as an increase of extreme flood events from the Oglio. This is probably linked to higher sediment availability in the catchment. Only two periods of flood frequency increase are recorded between 1200 and 1880 cal CE : one between 1330 and 1430 cal CE that appears at the end of a period of high sedimentation rate, and the other one between 1500 and 1670 cal CE when a low maximum of 3 floods is recorded per 100 years. Flood frequency sharply increases after 1880 CE simultaneously with the last increase of remobilisation of previously deposited sediment in the deep basin and the increase of sedimentation rate, that reaches its maximum (> 5 $mm.yr^{-1}$). However, this last increase can also be due to the presence of eutrophic conditions at that time, inhibiting bioturbation processes and producing dark varved organic gyttja making easier the detection of light event layers on the top of the sediment section.

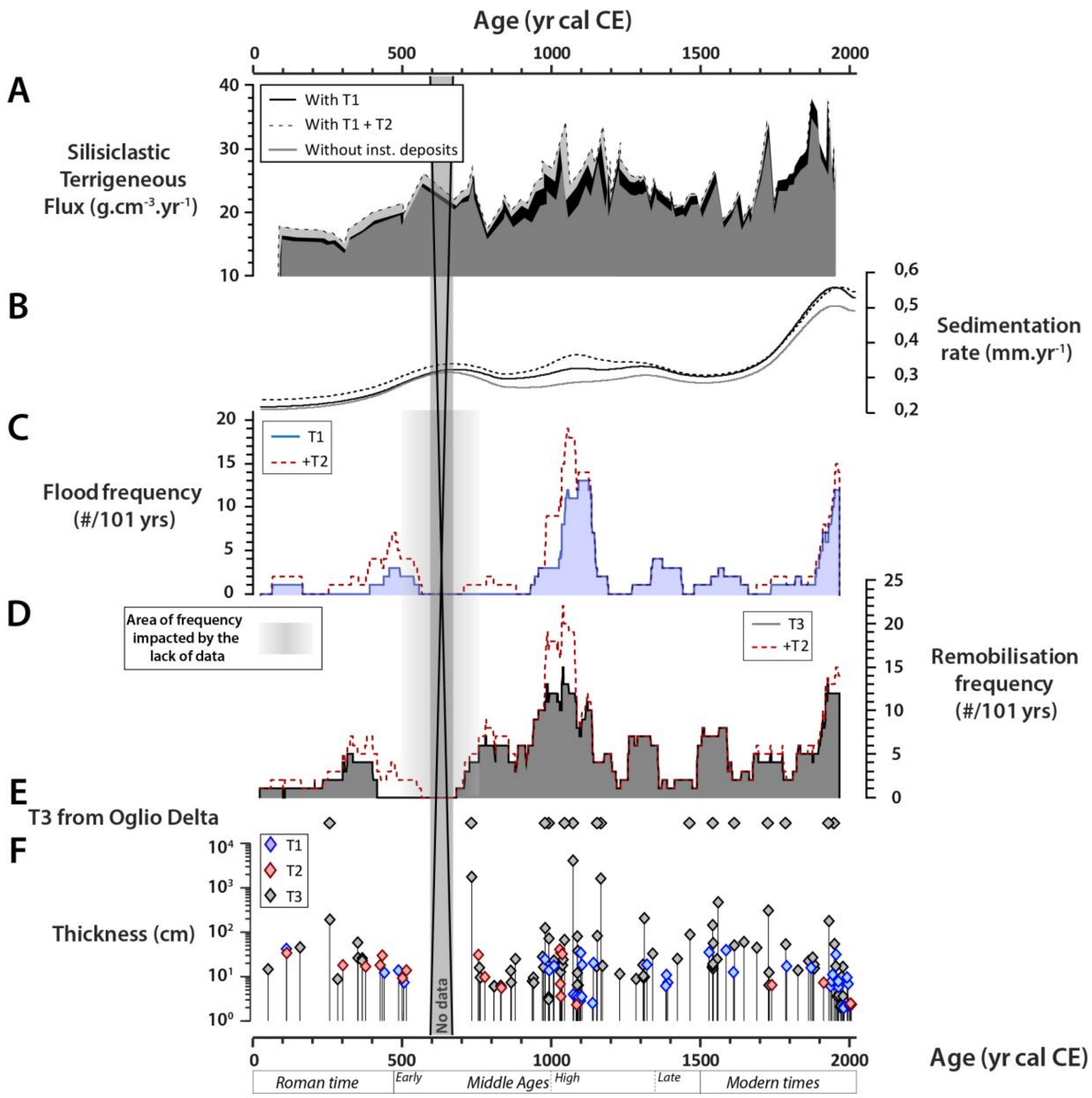

Figure 7 – Comparison of the main results obtained from the SEB18 sediment sequence plotted against the age. (A) SEB18 SCTF (B) SEB18 sedimentation rate, (C) flood frequency obtained from Type 1 layers ages, Type 1 and 2 sum is plotted in red dotted line, (D) remobilisation event frequency obtained from Type 3 layers ages, Type 3 and 2 sum is plotted in red dotted line, (E) Type 3 layers with a detrital composition, (F) the fluctuation of the thickness of each kind of layers. The area of frequency impacted by the lack of data is represented in grey shadings

5.4. Linking human-influence and sediment supply

The study of SEB18 sequence has allowed to link the occurrence of remobilisations of previously deposited sediment (Type 3) to the amount of sediment available in the lake basin. Parameters such as local and regional climate variability and the evolution of human activities in the watershed regulate the sediment input in a lake basin. Several studies have shown that human activities in the watershed can be the first forcing factor on the sediment supply in a lake (Bajard et al., 2016; Giguet-Covex et al., 2012; Joannin et al., 2014; Rapuc et al., 2019, 2018). This is especially true since the Roman times, when agricultural and pastoral activities were widely developed in Europe and often associated with deforestation (Andrič et al., 2020; Bajard et al., 2020, 2017a, 2017b; Giguet-Covex et al., 2014; Joannin et al., 2014). Thus, considering the geodynamic as a constant parameter during the last 2000 yrs, the impact of human activities and climate fluctuations on the sediment inputs in the deep basin of Lake Iseo and on the occurrence of remobilisation of previously deposited sediment needs to be established (**Fig. 8**).

5.4.1. Before 0 yr CE

Erosion in the Val Camonica is already important at the beginning of the Roman period: the SCTF recorded at the base of the SEB18 sequence presents values around 15 $g.cm^{-3}.yr^{-1}$ (**Fig. 8**). From the Iron Age, a high number of rock carvings and several Camuni cities are identified in the Southern part of the watershed, indicating that the Camuni society was well developed before Roman invasion (Anati, 2009; Anati and Cittadini, 1994; Casini and De Marinis, 2009). Several palynological records from the watershed indicate that agricultural activities first start around 4 ka cal BP associated with mid-altitude pastoralism from 3 ka cal BP (Pini, 2002; Pini et al., 2016). In the Insubrian Alps, and more generally in the Southern Alps, human-induced deforestation and fire activity have occurred from 4 ka cal BP and increased from the Late Iron Age (Comiti, 2012; Gobet et al., 2000; Iglesias et al., 2019). All of these evidences, associated with previous studies on lake sediment in the Southern and Julian Alps (Andrič et al., 2020; Joannin et al., 2014; Rapuc et al., 2019, 2018), suggest that human activities already impact the erosion and sediment transport processes in the main watersheds of the Southern Alps before the Roman Period.

5.4.2. Roman Period to Early Middle Ages

From the base of the SEB18 sequence and for the remainder of the Roman period, the erosion in the Val Camonica increase. A strong erosion state is reached between 500 and 750 cal CE. During this period, the extreme floods frequency from the Oglio river is low and a small rise in the frequency of the remobilisation events occurred (300 to 440 CE; **Fig. 8**). Agricultural activities in the Val Camonica increase during the Roman period as indicated by the appearance of chestnuts and walnuts and by the increase of anthropogenic indicators in a middle altitude site (Pini, 2002). Until 150 cal CE, the Southern Alps and Northern Italy are marked by a population rise (Cascio and Malanima, 2005; Comiti, 2012) associated with intense pastoralism practices (Carrer, 2015). However, the Roman civilisation adopted management plans to reduce the deforestation leading to a lower than expected human impact on the erosion of the high-Alpine valleys in Italy at that time (Comiti, 2012). It is even assumed that the population and deforestations progressively decrease from 200 cal CE in the Southern Alps until the migration period, around 500 cal CE (Büntgen et al., 2011; Comiti, 2012; Joannin et al., 2014; Tinner et al., 2003) making it difficult to link the increase of the sedimentation rate with human activities. Yet, several studies have shown that contrary to the general tendency in Europe, pastoral activities increase at the end of the Roman period (250 to 500 CE) in the Val Camonica (Allevato et al., 2013; Gehrig, 1997; Pini, 2002; Pini et al., 2016). Moreover, between 410 to 760 cal CE, intense deforestation linked to ore-extraction also occurs in mid-altitude sites in the Southern part of Val Camonica (Marziani and Citterio, 1999; Pini et al., 2016). Deforestation for building and land-use purposes are also recorded all over Europe from 500 to 800 cal CE (Büntgen et al., 2011; Tinner et al., 2003). During the Roman period, between 0 and 300 cal CE, Europe underwent a dry and warm period directly followed by a decrease of temperature anomalies until 600 cal CE (**Fig. 8**) and a peak of precipitation at 420 cal CE followed by a drier period until approximately 650 cal CE (Büntgen et al., 2011). From all these evidences, the watershed of Lake Iseo went through a period of stress linked to both climate, intense deforestation and pastoralism after 400 cal CE. It seems difficult to disentangle here the effect of climate and human activities, but this combination led to a progressive increase of erosion and of flood frequency in the Val Camonica also observed at this time in the Southern Alps (**Fig. 8,** Glur et al., 2013). This was also demonstrated in piedmont mega-fans where the aggradation and avulsions increase between 500 and 900 cal CE due to a regionally wetter climate (Comiti, 2012). This period of sediment accumulation, that have lasted until at least 750 cal CE in Lake Iseo, has increased sediment availability in the lake that in turn caused an increase of the sensitivity of the lake to record remobilisation events as observed around 750 cal CE.

5.4.3. Early and High Middle Ages

After 800 cal CE, the erosion increases until a first peak at 1000 cal CE followed by fluctuations within a high value range until 1300 cal CE and then a global decrease until 1500 cal CE. Three peaks are observed at 1000, 1170 and 1230 cal CE (**Fig. 8**). This period starting at the end of the Early Middle Ages to the end of the High Middle Ages presents strong developments of the societies in Europe, associated with economic and agricultural growths (Büntgen et al., 2011). From 900 cal CE, the population in Italy starts to increase until the great Plague (Cascio and Malanima, 2005). In the Southern Alps, several studies reported an increase of land use between 800 and 1300 cal CE (Joannin et al., 2014; Paladin et al., 2020; Ravazzi et al., 2013). In the Val Camonica, this period exhibits a development of the agricultural activities at mid-altitude sites (Pini, 2002) with an increase of *Plantago* and *Artemisia* taxons. This agricultural growth is accompanied by the replacement of pre-existing structures from 900 cal CE in Europe (Büntgen et al., 2011). Altogether, these societal developments are at the origin of a period of intense deforestation between 800 and 1400 cal CE visible in Europe (Büntgen et al., 2011), South to Lake Garda (Ravazzi et al., 2013) and also in the watershed of Lake Iseo between 1170 and 1280 CE (Gehrig, 1997; Marziani and Citterio, 1999; Pini, 2002; Pini et al., 2016). There is no information that indicates a forest management in the Southern Alps at that period (Comiti, 2012), and the increase in erosion (**Fig. 8A**) suggests an important impact of the deforestation on the transport of sediment from the watershed to Lake Iseo. In Europe, an increase in the amount of precipitation is observed from 540 to 750 cal CE and is followed by a period of high precipitation lasting until approximately 960 cal CE (Büntgen et al., 2011). According to summer temperatures measured from tree rings, Europe experienced a warmer period from 800 to 1250 cal CE, known as the Medieval Warm Period. The climatic influence on the erosion processes in Lake Iseo watershed cannot be excluded, however, few floods are recorded in Southern Alps at that time (**Fig. 8**; Glur et al., 2013) making climatic impact on sediment transport during the Early and High Middle Ages less probable. The important human activity in the watershed through deforestation and land use allowed an increase of the erosion from 800 cal CE that led to intense sediment input in Lake Iseo probably helped by the increase of precipitation amount at that time in Europe. Flood frequency recorded in Lake Iseo starts to increase until 1200 CE, reaching a peak of 13 flood per century at 1120 CE, corresponding to the highest value of the chronicle (**Fig. 8**). This phenomenon is decorrelated from precipitation amounts in Europe, as they show decrease tendency from 960 CE (**Fig. 8**) and can only be due to the increase of sediment availability in the watershed after human-induced intense erosion. As a previous sediment accumulation period already occurred in Lake Iseo, the sensitivity of the lake was high, which explains the sudden increase of the remobilisation frequency from 880 cal CE and lasting until 1130 cal CE. The decrease of the remobilisation frequency after 1130 CE is not linked to a decrease of sediment input as erosion remains high after that time (**Fig. 8**). This decrease is more probably due to a decrease of the sediment available from the delta to the deep basin after the two main seismic events recorded at 1117 and 1222 CE.

5.4.4. Late Middle Ages and Little Ice Age

Between 1347 and 1351 cal CE, the Great Plague impacted all of Europe, causing the death of almost half of the population (Büntgen et al., 2011). This event led to a sharp decrease of the population in Italy lasting until 1500 cal CE (Cascio and Malanima, 2005). An important abandonment of agricultural practices appears at that time and led to partial reforestations, notably around Lake Ledro (Joannin et al., 2014). This has increased the stability of the hillslopes in the Southern Alps reducing the sediment mobilization by the rivers. In Val Camonica, there is no evidence of deforestation or intense human activities from 1280 CE (Pini et al., 2016). The sediments recorded in the deep basin of Lake Iseo show a decrease in erosion from 1230 until 1450 cal CE (**Fig. 8**). There is no evidence of a decrease of the precipitation amount (Büntgen et al., 2011) or in flood frequency (Glur et al., 2013) that might explain a reduction of erosion linked to the regional climate (**Fig. 8**). At that time, decrease in erosion recorded in SEB18 section is linked to the decrease of human activity in Val Camonica. The increase of remobilisation events recorded between 1260 and 1350 cal CE is only due to destabilisation of the lake slopes, the Oglio delta being depleted in sediment from the last big seismic event of 1222 CE (**Fig. 7**).

After 1440 cal CE, a new period of intense deforestation for ore extraction is recorded in Val Camonica (Marziani and Citterio, 1999) that lasted until ~1700 cal CE. This deforestation is also visible across Europe and linked more generally to a recovery of human activities and land use after the Great Plague (Büntgen et al., 2011). After 1500 cal CE and until the end of the Little Ice Age (LIA), the precipitation amount across Europe and in the Alps increases simultaneously with a decrease of the temperature. This led to natural reforestation in uninhabited areas (e.g. Joannin et al., 2014). However, in the Southern Alps, the hillslopes instability increases due to climate-induced glaciers advances in high elevation during the LIA (Le Roy et al., 2015) associated with human exploitation of the forest (Fouinat et al., 2018), leading to an increase of erosion in Alpine watersheds and channel aggradation in the Po plain between 1600 and 1800 cal CE (Comiti, 2012). Until 1688 cal CE, there was no plan of forest management in the Italian Alps that could have prevent erosion (Comiti, 2012). The recovery of human activities in the Southern Alps associated with higher precipitation rates during the LIA are at the origin of the increase of detrital input in Lake Iseo, indicated by increasing erosional proxy starting around 1650 cal CE (**Fig. 8**).

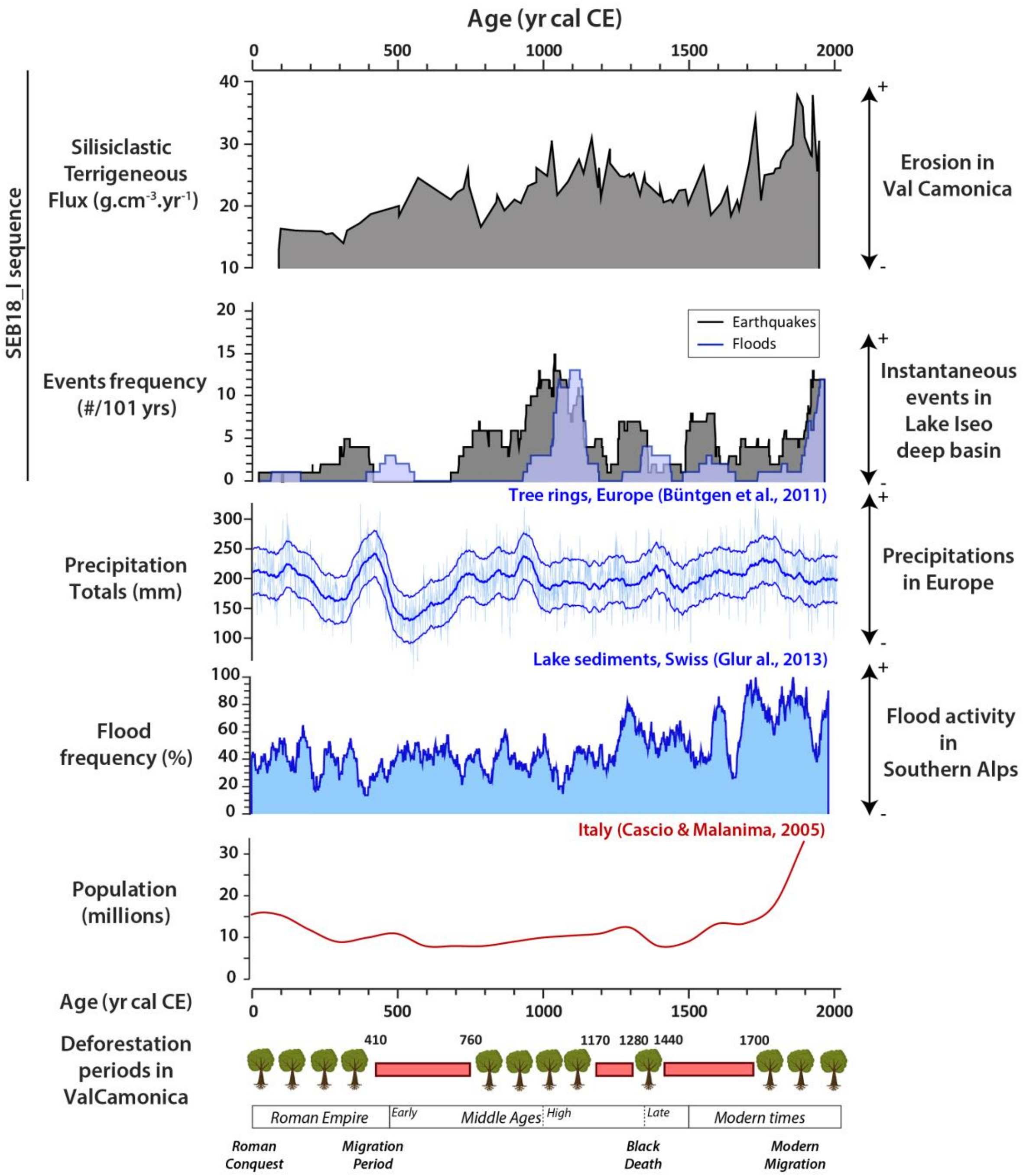

Figure 8 - Comparison between SEB18 SCTF, flood frequency and remobilisation event frequency obtained from Type 1 and Type 3 layers ages, respectively, reconstructed AMJ precipitation totals, modified from Büntgen et al., 2011 , 50-year moving average of flood events from Swiss lakes, modified from Glur et al., 2013, evolution of the population in Italy, expressed in million, modified from Cascio and Malanima, 2005, and periods of deforestation in the Iseo watershed deduced from Marziani and Citterio, 1999; Pini, 2002 and Pini et al., 2016.

5.4.5. Recent Times

The highest erosion recorded in the deep basin of Lake Iseo is reached at 1880 cal CE and corresponds to the end of the LIA. The sedimentation rate and extreme flood frequency continue to increase until 1950 cal CE. This can be attributed to a continuous remobilisation of the sediment derived from glaciers advances and hillslopes destabilisation in the upper part of the alpine catchments during the LIA (Comiti, 2012). Moreover, forest covers are low in the Southern Alps until the end of the World War I and the first emigration of the twentieth century of Italian people (Comiti, 2012). The period between the two World Wars corresponds to a time of decrease of land-use and agricultural activities in the Italian Alps due to emigration (Comiti, 2012). The catchment erosion as recorded in Lake Iseo only starts to decrease in the middle of the twentieth century probably due to (i) the decrease of precipitation amount from the end of the LIA, (ii) a global development of forest management, and also (iii) the creation of dams on the Oglio river starting around 1920 CE. However, as the detrital input in the deep basin was critical until the end of the nineteenth century, the load of sediment on the slopes and on the deltas was high, leading to an increase of the sensitivity of the lake to record seismic shaking explaining the increase of the remobilisation frequency recorded from 1800 to 1950 cal CE. Even if less sediment can be transported after 1950 cal CE due to intense damming of the Alpine rivers such as the Oglio river, the flood frequency recorded in the deep basin sharply increases after 1890 cal CE. From 1950 CE, the eutrophication of the lake makes easier the detection of small light grey detrital layers in a brown organic-rich sediment. High values of flood frequency at that time can then also be an artefact. This is supported by the small size of floods recorded at that period (**Fig. 7F**).

5.5. Human-influence on erosion and transport processes

The comparison between the sediment sequence retrieved in the deep basin of Lake Iseo and the knowledge of geodynamic, climate and human activities throughout the last 2000 years in the Italian Southern Alps helped to understand the drivers of the sediment inputs through erosion into the deep basin of Lake Iseo. It appears that from the Roman Period, human activities, by expanding grazing, by increasing agricultural activities and deforestations have induced a general destabilization of slopes and an increase in sediment input towards depositional sinks (**Fig. 9**). After a delay due to transport processes, the increased amount of sediment brought to intermediate sinks is stocked on lakes deltas and slopes. This abnormal sediment accumulation lead to an increase of the sedimentation rate in lakes deep basins and, after periods of high sediment input, cause an increase of destabilisation of slopes or deltas due to seismic shaking or sediment overloading. Equally, due to increase sediment availability in lakes catchments, the sediment load during a flood event will increase, leading to an increase of flood frequency recorded in lake sediments independent of climate fluctuations (**Fig. 9**). Then, even in large lake catchments, human activities through deforestation, pastoralism, and agriculture, affect the CZ by increasing erosion and resulting sediment transport and remobilization. This directly impacts the sensitivity of a lake as a natural archive to record the functioning of the CZ. Lastly, the increase of sediment availability by human activity cause a disconnection between the recorded instantaneous event frequency from the occurrence of their geodynamical triggering mechanisms.

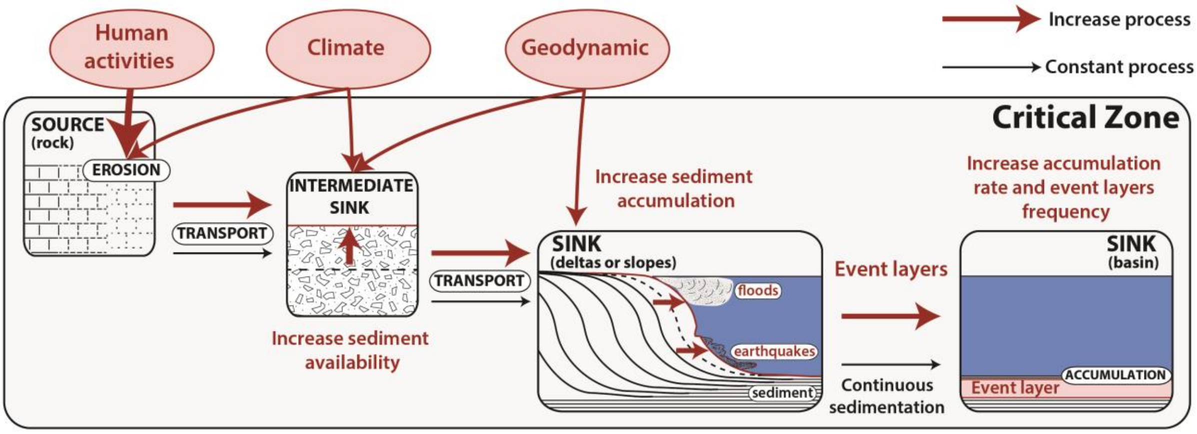

Figure 9 – Conceptual model of the CZ erosion cycle in a large catchment and the effects of the three main forcing factors (human activities, climate and geodynamic). Modified from Arnaud et al. (2016).

6. Conclusion

In this study, we have presented the first high-resolution record of the continuous and event layer sedimentation in a deep basin of a large peri-Alpine lake over the last 2000 years. In a large and deep lake, a lot of different sources can influence the sediment deposited in the deep basin making it more difficult to disentangle the processes that produce event layers. Only a multi-proxy approach associated to seismic survey allows to understand in detail the sedimentation of a large lake. To classify all event layers, we used XRF ratios, namely i) Ca/Sr ratio as a proxy of sediment source, to distinguish detrital input from sediment enriched in authigenic carbonates, and ii) Zr/K ratio associated with the thickness of each layer as proxies of transport processes. Three types of event layers were identified, the first one is defined by layers with a detrital composition associated with a high grain-size. This type is interpreted as caused by turbiditic currents related to underflow during extreme flood events, and ages of recent layers match with local historical flood events. The origin of the second type of layers could not be defined. The last one presents sediments from the slopes or the delta remobilized by slides in relation to sediment overloading or to seismic shaking. The ages of two on three largest layers, with considerable sediment volume amount, match with historical earthquakes of 1065 or 1117, and 1222 CE, supporting our interpretation.

It appears that the frequency of remobilisation events in Lake Iseo is directly linked to the sediment available on delta to be remobilized in the deep basin which depends on the erosion rate in the catchment. The variation in sediment input and the frequency of the remobilisation events in the deep basin of Lake Iseo with the study of different CZ forcing factors allowed to evidence that human activities in the watershed are the main driver through erosion processes at least from the Roman Period. Human practices and, to a lesser extent, climate fluctuations have impacted the available sediment in the lake and thus the recording of extreme geodynamic events. Hence, even in large catchments, human activities play a key role on erosion processes and on sediment availability, disrupting the recording of the CZ functioning in such archive.

Acknowledgements

This work was conducted in the framework of the CRITLAKE project funded by the AAP Université Savoie Mont Blanc in 2018 and thanks to the support of the entire staff of the C2FN-DT-INSU associated to the CLIMCORE project. Thanks to Qi Lin for his support and great help on the coring survey. Thanks to the Associazione Nazionale dei Carabinieri (Cesare Miniaci, Michele Liso, and colleagues) for the assistance on the lake, the use of their boat for the seismic survey and the anchoring of the platform. 14C analyses were acquired thanks to the CNRS-INSU ARTEMIS national radiocarbon AMS measurement programme at Laboratoire de Mesure 14C (LMC14) in the CEA Institute at Saclay (French Atomic Energy Commission). Thanks to Kim Genuite for the valuable help with GIS processing and the creation of the maps. Thanks to Lucilla Benedetti, Roberta Pini, Giulia Valerio and Marco Pilotti for their helpful advices. Thanks to Christian Crouzet for his help in the understanding of transport processes at the origin of the main layers

References

Allevato, E., Fedele, F., Terrasi, F., Capano, M., Pasquale, G.D., 2013. High-Resolution Archaeoenvironmental Study of a Cultic Episode at a Statue-Menhir Copper Age Site (Ossimo Anvòia, Italian Alps). Radiocarbon 55, 49–58. https://doi.org/10.2458/azu_js_rc.v55i1.16063

Ambrosetti, W., Barbanti, L., 2005. Evolution towards meromixis of Lake Iseo (Northern Italy) as revealed by its stability trend. J. Limnol. 64, 1. https://doi.org/10.4081/jlimnol.2005.1

Anati, E., 2009. L'art rupestre du Valcamonica : évolution et signification. Une vision panoramique d'après l'état actuel de la recherche. L'Anthropologie, Représentations préhistoriques. Images du sens (3/3) 113, 930–968. https://doi.org/10.1016/j.anthro.2009.10.003

Anati, E., Cittadini, T., 1994. Valcamonica rock art: a new history for Europe.

Andrič, M., Sabatier, P., Rapuc, W., Ogrinc, N., Dolenec, M., Arnaud, F., von Grafenstein, U., Šmuc, A., 2020. 6600 years of human and climate impacts on lake-catchment and vegetation in the Julian Alps (Lake Bohinj, Slovenia). Quat. Sci. Rev. 227, 106043. https://doi.org/10.1016/j.quascirev.2019.106043

Arnaud, F., 2005. Discriminating bio-induced and detrital sedimentary processes from particle size distribution of carbonates and non-carbonates in hard water lake sediments. J. Paleolimnol. 34, 519–526.

Arnaud, F., Poulenard, J., Giguet-Covex, C., Wilhelm, B., Révillon, S., Jenny, J.-P., Revel, M., Enters, D., Bajard, M., Fouinat, L., others, 2016. Erosion under climate and human pressures: An alpine lake sediment perspective. Quat. Sci. Rev. 152, 1–18.

Bajard, M., Poulenard, J., Sabatier, P., Bertrand, Y., Crouzet, C., Ficetola, G.F., Blanchet, C., Messager, E., Giguet-Covex, C., Gielly, L., Rioux, D., Chen, W., Malet, E., Develle, A.-L., Arnaud, F., 2020. Pastoralism increased vulnerability of a subalpine catchment to flood hazard through changing soil properties. Palaeogeogr. Palaeoclimatol. Palaeoecol. 538, 109462. https://doi.org/10.1016/j.palaeo.2019.109462

Bajard, M., Poulenard, J., Sabatier, P., Develle, A.-L., Giguet-Covex, C., Jacob, J., Crouzet, C., David, F., Pignol, C., Arnaud, F., 2017a. Progressive and regressive soil evolution phases in the Anthropocene. Catena 150, 39–52.

Bajard, M., Poulenard, J., Sabatier, P., Etienne, D., Ficetola, F., Chen, W., Gielly, L., Taberlet, P., Develle, A.-L., Rey, P.-J., 2017b. Long-term changes in alpine pedogenetic processes: Effect of millennial agro-pastoralism activities (French-Italian Alps). Geoderma 306, 217–236.

Bajard, M., Sabatier, P., David, F., Develle, A.-L., Reyss, J.-L., Fanget, B., Malet, E., Arnaud, D., Augustin, L., Crouzet, C., Poulenard, J., Arnaud, F., 2016. Erosion record in Lake La Thuile sediments (Prealps, France): Evidence of montane landscape dynamics throughout the Holocene. The Holocene 26, 350–364. https://doi.org/10.1177/0959683615609750

Banwart, S.A., Chorover, J., Gaillardet, J., Sparks, D., White, D., Anderson, S., Aufdenkampe, A., Bernasconi, S., Brantley, S.L., Chadwick, O., Dietrich, W.E., Duffy, C., Goldhaber, M.B., Lehnert, K., Nikolaidis, N.P., Ragnarsdottir, K.V., 2013. Sustaining Earth's Critical ZoneBasic Science and Interdisciplinary Solutions for Global Challenges. The University of Sheffield, United Kingdom.

Benedetti, L., Manighetti, I., Gaudemer, Y., Finkel, R., Malavieille, J., Pou, K., Arnold, M., Aumaître, G., Bourlès, D., Keddadouche, K., 2013. Earthquake synchrony and clustering on Fucino faults (Central Italy) as revealed from in situ 36Cl exposure dating. J. Geophys. Res. Solid Earth 118, 4948–4974. https://doi.org/10.1002/jgrb.50299

Bini, A., Cita, M.B., Gaetani, M., 1978. Southern Alpine Lakes—Hypothesis of an erosional origin related to the Messinian entrenchment. Mar. Geol. 27, 271–288.

Bini, A., Corbari, D., Falletti, P., Fassina, M., Perotti, C.R., Piccin, A., 2007. Morphology and geological setting of Iseo Lake (Lombardy) through multibeam bathymetry and high-resolution seismic profiles. Swiss J. Geosci. 100, 23–40.

Blaauw, M., 2010. Methods and code for 'classical'age-modelling of radiocarbon sequences. Quat. Geochronol. 5, 512–518.

Blass, A., Anselmetti, F.S., Grosjean, M., Sturm, M., 2005. The last 1300 years of environmental history recorded in the sediments of Lake Sils (Engadine, Switzerland). Eclogae Geol. Helvetiae 98, 319–332. https://doi.org/10.1007/s00015-005-1166-5

Brisset, E., Guiter, F., Miramont, C., Troussier, T., Sabatier, P., Poher, Y., Cartier, R., Arnaud, F., Malet, E., Anthony, E.J., 2017. The overlooked human influence in historic and prehistoric floods in the European Alps. Geology 45, 347–350.

Brown, R.J., Severin, K.P., 2009. Otolith chemistry analyses indicate that water Sr:Ca is the primary factor influencing otolith Sr:Ca for freshwater and diadromous fish but not for marine fish. Can. J. Fish. Aquat. Sci. 66, 1790–1808. https://doi.org/10.1139/F09-112

Bruel, R., Marchetto, A., Bernard, A., Lami, A., Sabatier, P., Frossard, V., Perga, M.-E., 2018. Seeking alternative stable states in a deep lake. Freshw. Biol. 63, 553–568.

Büntgen, U., Tegel, W., Nicolussi, K., McCormick, M., Frank, D., Trouet, V., Kaplan, J.O., Herzig, F., Heussner, K.-U., Wanner, H., Luterbacher, J., Esper, J., 2011. 2500 Years of European Climate Variability and Human Susceptibility. Science 331, 578–582. https://doi.org/10.1126/science.1197175

Carrer, F., 2015. Herding Strategies, Dairy Economy and Seasonal Sites in the Southern Alps: J. Mediterr. Archaeol. 28, 3–22. https://doi.org/10.1558/jmea.v28i1.27499

Cascio, E.L., Malanima, P., 2005. Cycles and Stability. Italian Population before the Demographic Transition (225 B.C. - A.D. 1900). Riv. Storia Econ. https://doi.org/10.1410/20933

Casini, S., De Marinis, R., 2009. Des pierres et des dieux. L'art rupestre de la Valteline et du Valcamonica. Globe Rev. Genevoise Géographie 149, 61–92. https://doi.org/10.3406/globe.2009.1556

Chapron, E., Simonneau, A., Ledoux, G., Arnaud, F., Lajeunesse, P., Albéric, P., 2016. French Alpine Foreland Holocene Paleoseismicity Revealed by Coeval Mass Wasting Deposits in Glacial Lakes, in: Submarine Mass Movements and Their Consequences. Springer, pp. 341–349.

Comiti, F., 2012. How natural are Alpine mountain rivers? Evidence from the Italian Alps. Earth Surf. Process. Landf. 37, 693–707. https://doi.org/10.1002/esp.2267

Condina, F.A., 1986. Carta archeologica della media e bassa Val Camonica: F. 34-Breno. Ed." Quaderni Camuni".

Cuven, S., Francus, P., Lamoureux, S., 2011. Mid to Late Holocene hydroclimatic and geochemical records from the varved sediments of East Lake, Cape Bounty, Canadian High Arctic. Quat. Sci. Rev. 30, 2651–2665. https://doi.org/10.1016/j.quascirev.2011.05.019

Cuven, S., Francus, P., Lamoureux, S.F., 2010. Estimation of grain size variability with micro X-ray fluorescence in laminated lacustrine sediments, Cape Bounty, Canadian High Arctic. J. Paleolimnol. 44, 803–817.

DISS Working Group, 2018. Database of Individual Seismogenic Sources (DISS), version 3.2.1.

Doyen, É., Vannière, B., Berger, J.-F., Arnaud, F., Tachikawa, K., Bard, E., 2013. Land-use changes and environmental dynamics in the upper Rhone valley since Neolithic times inferred from sediments in Lac Moras. The Holocene 23, 961–973. https://doi.org/10.1177/0959683612475142

Edwards, K.J., Whittington, G., 2001. Lake sediments, erosion and landscape change during the Holocene in Britain and Ireland. CATENA, Landscape sensitivity: principles and applications in Northern 42, 143–173. https://doi.org/10.1016/S0341-8162(00)00136-3

Fanetti, D., Anselmetti, F.S., Chapron, E., Sturm, M., Vezzoli, L., 2008. Megaturbidite deposits in the Holocene basin fill of Lake Como (southern Alps, Italy). Palaeogeogr. Palaeoclimatol. Palaeoecol. 259, 323–340.

Faure, G., Crocket, J.H., Hueley, P.M., 1967. Some aspects of the geochemistry of strontium and calcium in the Hudson Bay and the Great Lakes. Geochim. Cosmochim. Acta 31, 451–461. https://doi.org/10.1016/0016-7037(67)90053-1

Fouinat, L., Sabatier, P., David, F., Montet, X., Schoeneich, P., Chaumillon, E., Poulenard, J., Arnaud, F., 2018. Wet avalanches: long-term evolution in the Western Alps under climate and human forcing. Clim. Past 14.

Fouinat, L., Sabatier, P., Poulenard, J., Etienne, D., Crouzet, C., Develle, A.-L., Doyen, E., Malet, E., Reyss, J.-L., Sagot, C., Bonet, R., Arnaud, F., 2017. One thousand seven hundred years of interaction between glacial activity and flood frequency in proglacial Lake Muzelle (western French Alps). Quat. Res. 87, 407–422. https://doi.org/10.1017/qua.2017.18

Galadini, F., Galli, P., Molin, D., Ciurletti, G., 2001. Searching for the Source of the 1117 Earthquake in Northern Italy: A Multidisciplinary Approach, in: Glade, T., Albini, P., Francés, F. (Eds.), The Use of Historical Data in Natural Hazard Assessments. Springer Netherlands, Dordrecht, pp. 3–27. https://doi.org/10.1007/978-94-017-3490-5_1

Garibaldi, L., Mezzanotte, V., Brizzio, M.C., Rogora, M., Mosello, R., 1999. The trophic evolution of Lake Iseo as related to its holomixis. J. Limnol. 58, 10. https://doi.org/10.4081/jlimnol.1999.10

Gasperini, P., Camassi, R., Mirto, C., Stucchi, M., 2004. Catalogo Parametrico dei Terremoti Italiani, versione CPTI04. Istituto Nazionale di Geofisica e Vulcanologia (INGV).

Gehrig, R., 1997. Pollenanalytische Untersuchungen zur Vegetations-und-Klimageschichte des Val Camonica (Norditalien).

Giardini, D., Woessner, J., Danciu, L., Crowley, H., Cotton, F., Grünthal, G., Pinho, R., Valensise, G., Akkar, S., Arvidsson, R., 2013. Seismic hazard harmonization in Europe (SHARE): online data resource. Swiss Seism Serv ETH Zurich Zurich Switz Doi 10.

Giguet-Covex, C., Arnaud, F., Enters, D., Poulenard, J., Millet, L., Francus, P., David, F., Rey, P.-J., Wilhelm, B., Delannoy, J.-J., 2012. Frequency and intensity of high-altitude floods over the last 3.5 ka in northwestern French Alps (Lake Anterne). Quat. Res. 77, 12–22.

Giguet-Covex, C., Arnaud, F., Poulenard, J., Disnar, J.-R., Delhon, C., Francus, P., David, F., Enters, D., Rey, P.-J., Delannoy, J.-J., 2011. Changes in erosion patterns during the Holocene in a currently treeless subalpine catchment inferred from lake sediment geochemistry (Lake Anterne, 2063 m asl, NW French Alps): the role of climate and human activities. The Holocene 0959683610391320.

Giguet-Covex, C., Pansu, J., Arnaud, F., Rey, P.-J., Griggo, C., Gielly, L., Domaizon, I., Coissac, E., David, F., Choler, P., Poulenard, J., Taberlet, P., 2014. Long livestock farming history and human landscape shaping revealed by lake sediment DNA. Nat. Commun. 5, 1–7. https://doi.org/10.1038/ncomms4211

Glover, T.J., 1997. Pocket Ref, 2nd ed. Sequoia, Littleton, Colo.

Glur, L., Wirth, S.B., Büntgen, U., Gilli, A., Haug, G.H., Schär, C., Beer, J., Anselmetti, F.S., 2013. Frequent floods in the European Alps coincide with cooler periods of the past 2500 years. Sci. Rep. 3, 2770.

Gobet, E., Tinner, W., Hubschmid, P., Jansen, I., Wehrli, M., Ammann, B., Wick, L., 2000. Influence of human impact and bedrock differences on the vegetational history of the Insubrian Southern Alps. Veg. Hist. Archaeobotany 9, 175–187. https://doi.org/10.1007/BF01299802

Guidoboni, E., Comastri, A., Boschi, E., 2005. The “exceptional” earthquake of 3 January 1117 in the Verona area (northern Italy): A critical time review and detection of two lost earthquakes (lower Germany and Tuscany). J. Geophys. Res. Solid Earth 110.

Guzzetti, F., Tonelli, G., 2004. Information system on hydrological and geomorphological catastrophes in Italy (SICI): a tool for managing landslide and flood hazards. Nat. Hazards Earth Syst. Sci. 4, 213–232.

Hieke, W., 1984. A thick Holocene homogenite from the Ionian Abyssal Plain (eastern Mediterranean). Mar. Geol. 55, 63–78. https://doi.org/10.1016/0025-3227(84)90133-6

Hogg, C.A., Marti, C.L., Huppert, H.E., Imberger, J., 2013. Mixing of an interflow into the ambient water of Lake Iseo. Limnol. Oceanogr. 58, 579–592.

Iglesias, V., Vannière, B., Jouffroy-Bapicot, I., 2019. Emergence and Evolution of Anthropogenic Landscapes in the Western Mediterranean and Adjacent Atlantic Regions. Fire 2, 53. https://doi.org/10.3390/fire2040053

Joannin, S., Magny, M., Peyron, O., Vannière, B., Galop, D., 2014. Climate and land-use change during the late Holocene at Lake Ledro (southern Alps, Italy). The Holocene 24, 591–602.

Kastens, K.A., Cita, M.B., 1981. Tsunami-induced sediment transport in the abyssal Mediterranean Sea. GSA Bull. 92, 845–857. https://doi.org/10.1130/0016-7606(1981)92<845:TSTITA>2.0.CO;2

Kylander, M.E., Ampel, L., Wohlfarth, B., Veres, D., 2011. High-resolution X-ray fluorescence core scanning analysis of Les Echets (France) sedimentary sequence: new insights from chemical proxies. J. Quat. Sci. 26, 109–117. https://doi.org/10.1002/jqs.1438

Lauterbach, S., Chapron, E., Brauer, A., Hüls, M., Gilli, A., Arnaud, F., Piccin, A., Nomade, J., Desmet, M., Von Grafenstein, U., 2012. A sedimentary record of Holocene surface runoff events and earthquake activity from Lake Iseo (Southern Alps, Italy). The Holocene 22, 749–760.

Le Roy, M., Nicolussi, K., Deline, P., Astrade, L., Edouard, J.-L., Miramont, C., Arnaud, F., 2015. Calendar-dated glacier variations in the western European Alps during the Neoglacial: the Mer de Glace record, Mont Blanc massif. Quat. Sci. Rev. 108, 1–22. https://doi.org/10.1016/j.quascirev.2014.10.033

Livio, F.A., Berlusconi, A., Michetti, A.M., Sileo, G., Zerboni, A., Trombino, L., Cremaschi, M., Mueller, K., Vittori, E., Carcano, C., Rogledi, S., 2009. Active fault-related folding in the epicentral area of the December 25, 1222 (Io=IX MCS) Brescia earthquake (Northern Italy): Seismotectonic implications. Tectonophysics, Ten years after the Umbria-Marche earthquake, Central Italy 476, 320–335. https://doi.org/10.1016/j.tecto.2009.03.019

Luino, F., Belloni, A., Padovan, N., Bassi, M., Bossuto, P., Fassi, P., 2002. Historical and geomorphological analysis as a research tool for the identification of flood-prone zones and its role in the revision of town planning: the Oglio basin (Valcamonica–Northern Italy), in: 9th Congress of the International Association for Engineering Geology and the Environment, Edited by: Van Rooy, JL and Jermy, CA, Durban (South Africa). pp. 16–20.

Marziani, G., Citterio, S., 1999. The effects of human impact on the arboreal vegetation near ancient iron smelting sites in Val Gabbia, northern Italy. Veg. Hist. Archaeobotany 8, 225–229. https://doi.org/10.1007/BF02342722

Paladin, A., Moghaddam, N., Stawinoga, A.E., Siebke, I., Depellegrin, V., Tecchiati, U., Lösch, S., Zink, A., 2020. Early medieval Italian Alps: reconstructing diet and mobility in the valleys. Archaeol. Anthropol. Sci. 12, 82. https://doi.org/10.1007/s12520-019-00982-6

Piaz, G.V.D., Bistacchi, A., Massironi, M., 2003. Geological outline of the Alps. Episodes 26, 175–180. https://doi.org/10.18814/epiiugs/2003/v26i3/004

Pilotti, M., Valerio, G., Giardino, C., Bresciani, M., Chapra, S.C., 2018. Evidence from field measurements and satellite imaging of impact of Earth rotation on Lake Iseo chemistry. J. Gt. Lakes Res. 44, 14–25. https://doi.org/10.1016/j.jglr.2017.10.005

Pilotti, M., Valerio, G., Leoni, B., 2013. Data set for hydrodynamic lake model calibration: A deep prealpine case. Water Resour. Res. 49, 7159–7163.

Pini, R., 2002. A high-resolution Late-Glacial – Holocene pollen diagram from Pian di Gembro (Central Alps, Northern Italy). Veg. Hist. Archaeobotany 11, 251–262. https://doi.org/10.1007/s003340200038

Pini, R., Ravazzi, C., Aceti, A., Castellano, L., Perego, R., Quirino, T., Valle', F., 2016. Ecological changes and human interaction in Valcamonica, the rock art valley, since the last deglaciation 29, 19–34.

Ramisch, F., Dittrich, M., Mattenberger, C., Wehrli, B., Wüest, A., 1999. Calcite dissolution in two deep eutrophic lakes. Geochim. Cosmochim. Acta 63, 3349–3356. https://doi.org/10.1016/S0016-7037(99)00256-2

Rapuc, W., Sabatier, P., Andrič, M., Crouzet, C., Arnaud, F., Chapron, E., Šmuc, A., Develle, A.-L., Wilhelm, B., Demory, F., 2018. 6600 years of earthquake record in the Julian Alps (Lake Bohinj, Slovenia). Sedimentology 65, 1777–1799.
Rapuc, W., Sabatier, P., Arnaud, F., Palumbo, A., Develle, A.-L., Reyss, J.-L., Augustin, L., Régnier, E., Piccin, A., Chapron, E., Dumoulin, J.-P., von Grafenstein, U., 2019. Holocene-long record of flood frequency in the Southern Alps (Lake Iseo, Italy) under human and climate forcing. Glob. Planet. Change 175, 160–172. https://doi.org/10.1016/j.gloplacha.2019.02.010
Ravazzi, C., Marchetti, M., Zanon, M., Perego, R., Quirino, T., Deaddis, M., De Amicis, M., Margaritora, D., 2013. Lake evolution and landscape history in the lower Mincio River valley, unravelling drainage changes in the central Po Plain (N-Italy) since the Bronze Age. Quat. Int., Quaternary in Italy: knowledge and perspective 288, 195–205. https://doi.org/10.1016/j.quaint.2011.11.031
Regattieri, E., Zanchetta, G., Isola, I., Zanella, E., Drysdale, R.N., Hellstrom, J.C., Zerboni, A., Dallai, L., Tema, E., Lanci, L., Costa, E., Magrì, F., 2019. Holocene Critical Zone dynamics in an Alpine catchment inferred from a speleothem multiproxy record: disentangling climate and human influences. Sci. Rep. 9, 17829. https://doi.org/10.1038/s41598-019-53583-7
Reimer, P.J., Bard, E., Bayliss, A., Beck, J.W., Blackwell, P.G., Bronk Ramsey, C., Buck, C.E., Cheng, H., Edwards, R.L., Friedrich, M., others, 2013. IntCal13 and Marine13 radiocarbon age calibration curves 0-50,000 years cal BP.
Rovida, A., Locati, M., Camassi, R., Lolli, B., Gasperini, P., 2020. The Italian earthquake catalogue CPTI15. Bull. Earthq. Eng. 18, 2953–2984. https://doi.org/10.1007/s10518-020-00818-y
Rovida, A.N., Locati, M., Camassi, R.D., Lolli, B., Gasperini, P., 2019. Catalogo Parametrico dei Terremoti Italiani CPTI15, versione 2.0 (report). https://doi.org/10.13127/CPTI/CPTI15.2
Sabatier, P., Dezileau, L., Briqueu, L., Colin, C., Siani, G., 2010. Clay minerals and geochemistry record from northwest Mediterranean coastal lagoon sequence: Implications for paleostorm reconstruction. Sediment. Geol. 228, 205–217.
Salmaso, N., Mosello, R., Garibaldi, L., Decet, F., Brizzio, M.C., Cordella, P., 2003. Vertical mixing as a determinant of trophic status in deep lakes: a case study from two lakes south of the Alps (Lake Garda and Lake Iseo). J. Limnol. 62, 33. https://doi.org/10.4081/jlimnol.2003.s1.33
Sauerbrey, M.A., Juschus, O., Gebhardt, A.C., Wennrich, V., Nowaczyk, N.R., Melles, M., 2013. Mass movement deposits in the 3.6 Ma sediment record of Lake El'gygytgyn, Far East Russian Arctic. Clim. Past 9, 1949–1967.
Serpelloni, E., Anzidei, M., Baldi, P., Casula, G., Galvani, A., 2005. Crustal velocity and strain-rate fields in Italy and surrounding regions: new results from the analysis of permanent and non-permanent GPS networks. Geophys. J. Int. 161, 861–880. https://doi.org/10.1111/j.1365-246X.2005.02618.x
Strasser, M., Monecke, K., Schnellmann, M., Anselmetti, F.S., 2013. Lake sediments as natural seismographs: A compiled record of Late Quaternary earthquakes in Central Switzerland and its implication for Alpine deformation. Sedimentology 60, 319–341.
Sturm, M., Matter, A., 1978. Turbidites and varves in Lake Brienz (Switzerland): deposition of clastic detritus by density currents. Wiley Online Library.
Tinner, W., Lotter, A.F., Ammann, B., Conedera, M., Hubschmid, P., van Leeuwen, J.F.N., Wehrli, M., 2003. Climatic change and contemporaneous land-use phases north and south of the Alps 2300 BC to 800 AD. Quat. Sci. Rev. 22, 1447–1460. https://doi.org/10.1016/S0277-3791(03)00083-0
Vannière, B., Magny, M., Joannin, S., Simonneau, A., Wirth, S.B., Hamann, Y., Chapron, E., Gilli, A., Desmet, M., Anselmetti, F.S., 2013. Orbital changes, variation in solar activity and increased anthropogenic activities: controls on the Holocene flood frequency in the Lake Ledro area, Northern Italy. Clim. Past 9, 1193–1209.
Verdecchia, A., Pace, B., Visini, F., Scotti, O., Peruzza, L., Benedetti, L., 2018. The Role of Viscoelastic Stress Transfer in Long-Term Earthquake Cascades: Insights After the Central Italy 2016–2017 Seismic Sequence. Tectonics 37, 3411–3428. https://doi.org/10.1029/2018TC005110

Wilhelm, B., Arnaud, F., Sabatier, P., Crouzet, C., Brisset, E., Chaumillon, E., Disnar, J.-R., Guiter, F., Malet, E., Reyss, J.-L., others, 2012. 1400years of extreme precipitation patterns over the Mediterranean French Alps and possible forcing mechanisms. Quat. Res. 78, 1–12.

Wilhelm, B., Arnaud, F., Sabatier, P., Magand, O., Chapron, E., Courp, T., Tachikawa, K., Fanget, B., Malet, E., Pignol, C., Bard, E., Delannoy, J.J., 2013. Palaeoflood activity and climate change over the last 1400 years recorded by lake sediments in the north-west European Alps. J. Quat. Sci. 28, 189–199. https://doi.org/10.1002/jqs.2609

Wilhelm, B., Nomade, J., Crouzet, C., Litty, C., Sabatier, P., Belle, S., Rolland, Y., Revel, M., Courboulex, F., Arnaud, F., others, 2016. Quantified sensitivity of small lake sediments to record historic earthquakes: implications for paleoseismology. J. Geophys. Res. Earth Surf. 121, 2–16.

Zádorová, T., Penížek, V., Šefrna, L., Drábek, O., Mihaljevič, M., Volf, Š., Chuman, T., 2013. Identification of Neolithic to Modern erosion–sedimentation phases using geochemical approach in a loess covered sub-catchment of South Moravia, Czech Republic. Geoderma 195–196, 56–69. https://doi.org/10.1016/j.geoderma.2012.11.012

Supplementary data

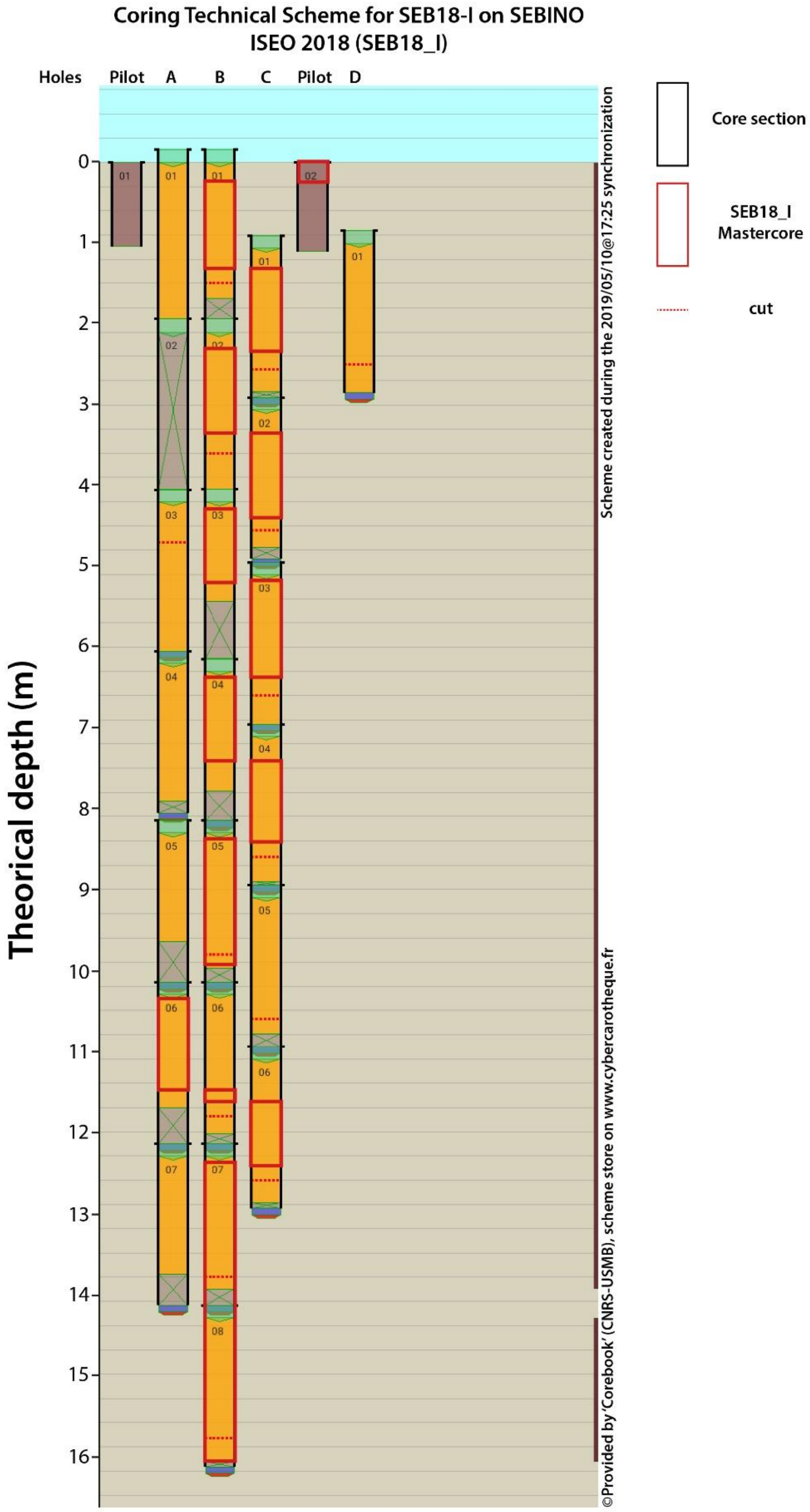

Supplementary Figure 1 – Coring technical scheme for SEB18_I sediment section. All cores retrieved from the deep basin during the SEB18_I coring survey are represented against a theorical depth (m). SEB18_I theorical sediment section is represented in red